Office of Naval Research
Contract Nonr-1866 (32) NR-371-016

A THEORETICAL STUDY OF DIELECTRIC-COATED CYLINDRICAL ANTENNAS

By
Chung-Yu Ting

July 1966

Technical Report No. 506

Division of Engineering and Applied Physics
Harvard University • Cambridge, Massachusetts

Office of Naval Research

Contract Nonr-1866(32)

NR - 371 - 016

A THEORETICAL STUDY OF DIELECTRIC-COATED CYLINDRICAL ANTENNAS

by

Chung-Yu Ting

Technical Report No. 506

July, 1966

The research reported in this document was made possible through support extended to Cruft Laboratory, Harvard University, by the U. S. Army Research Office, the U. S. Air Force Office of Scientific Services Electronics Program by Contract Nonr-1866(32).

Cruft Laboratory

Division of Engineering and Applied Physics

Harvard University

Cambridge, Massachusetts

A THEORETICAL STUDY OF DIELECTRIC-COATED CYLINDRICAL ANTENNAS

by

Chung-Yu Ting

Cruft Laboratory

Division of Engineering and Applied Physics

Harvard University, Cambridge, Massachusetts

ABSTRACT

A cylindrical antenna, either infinite or finite, which is imbedded in a concentric dielectric rod has been investigated by employing a rigorous formulation. The infinite case is solved easily by a Fourier transform method; the finite case is solved first by a numerical method, then by a two-term approximation. The mathematical analysis is intricate, nevertheless, the results obtained for the finite antenna are as simple as for the free-space dipole. It is shown in both cases that the input conductances are larger than for the corresponding free-space antennas, and the field patterns tend to be more broadside. The method is applicable regardless of the thicknesses of the antennas and the dielectric rod. This study is limited to thin antennas in rather thick dielectric cylinders. However, the dielectric rod is still not thick enough to support a T. M. mode.

I. INTRODUCTION

The problem of an antenna in a dielectric rod, sometimes called a dielectric-coated antenna has already been discussed by several investigators [1], [2]. As pointed out by Wu, when the coating and the antenna itself are very thin, the current distribution differs very little from that of a thin dipole in free space and can be put in a form equivalent to that for a thin dipole with a slightly modified radius and with a surface impedance. As the dielectric coating becomes thicker and thicker, changes are to be expected. For a very thick dielectric rod, the current in the antenna should behave more or less like that in a homogeneous dielectric medium. However, due to the complexity of the Green's function, an exact solution is very difficult to obtain.

In this study, an infinite cylindrical dielectric-coated antenna was investigated first. The current was expressed explicitly in an integral form and numerical values were calculated by computer. The contribution to the current from the simple pole, which is associated with the surface wave, is called the transmission current; the contribution from the branch cut, which is associated with the radiation field, is called the radiation current. Radiation patterns, radiation and transmission conductances, percentage power radiated and percentage power transmitted have been obtained. These results are useful in predicting some of the characteristics of a finite antenna.

Next, an exact integral equation for the current in a finite dipole in an infinitely long dielectric rod was formulated and solved

by a numerical method. The accuracy depends on the number of points taken and the accumulated round-off error. For a reasonable number of points the results show excellent agreement with experiments; they are consistent with the predictions made from the infinite antenna. That is, when the dielectric layer is thick the current is dominated by the transmission current. From this property, an approximate current can be found by a two-term method with a propagation constant equal to the surface wave number. The field pattern can be calculated more easily from this approximate current than from the numerical data.

II. INFINITE CYLINDRICAL DIELECTRIC-COATED ANTENNA

A. Boundary-Value Problem

Figure 1 shows a schematic diagram of an infinite cylindrical dielectric-coated antenna with a slice delta generator at $z=0$. Assume the antenna to be thin and rotational symmetry to be maintained, $\frac{\partial}{\partial\theta}=0$, so that only the z-components of current and vector potential are excited. By defining a vector potential and a scalar potential in the conventional way $\vec{B}=\nabla\times\vec{A}$, $\vec{E}=-\nabla\phi-\vec{A}$ and using the Lorentz-gauge condition $\nabla\cdot\vec{A}_1+\epsilon_1\mu_o\phi_1=0$ in region I, $\nabla\cdot\vec{A}_2+\epsilon_o\mu_o\phi_2=0$ in region II, where subscript 1 indicates quantities in region I; subscript 2 indicates quantities in region II, the wave equations of the one-component vector potentials $\vec{A}_z$ in the two regions become

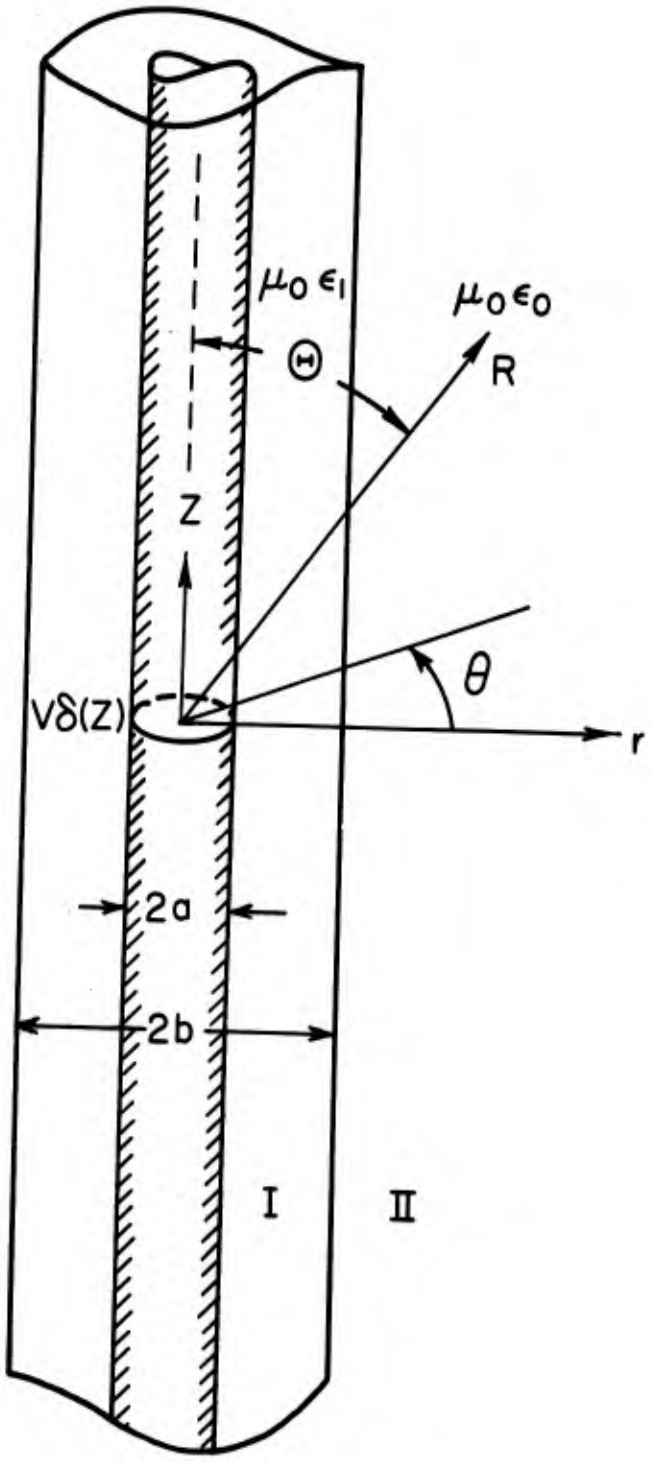

FIG. 1 A SCHEMATIC DIAGRAM OF A DIELECTRIC COATED INFINITE CYLINDRICAL ANTENNA WITH A DELTA GENERATOR AT $z = 0$

$$\nabla^2 A_{1z} + k_1^2 A_{1z} = 0 \qquad a \leqslant r < b \tag{1}$$

$$\nabla^2 A_{2z} + k_o^2 A_{2z} = 0 \qquad b < r < \infty \tag{2}$$

where ∇^2 is the Laplacian operator, $k_1 = \omega\sqrt{\mu_o \epsilon_1}$, $k_o = \omega\sqrt{\mu_o \epsilon_o}$ are, respectively, the wave numbers in the dielectric medium and in free space; ω is the angular frequency; μ_o and ϵ_o are the free-space permeability and dielectric constants; ϵ_1 and ϵ_r are the absolute dielectric constant and the relative dielectric constant in the dielectric medium so that $\epsilon_1 = \epsilon_r \epsilon_o$. The dielectric medium is assumed to have the same permeability as free space. After taking Fourier transforms of (1) and (2) with respect to z, according to the relations

$$\bar{F}(k) = \int_{-\infty}^{\infty} F(z)\, e^{ikz}\, dz \tag{3-a}$$

$$F(z) = \frac{1}{2\pi} \int_{-\infty}^{\infty} \bar{F}(k)\, e^{-ikz}\, dk \tag{3-b}$$

where $F(z)$ can be any field quantity, and $\bar{F}(k)$ is called the Fourier transform of $F(z)$. (1) and (2) become two Bessel equations. Solutions can be expressed in well-known cylindrical functions. They are

$$A_{1z} = C_1 J_o(\xi r) + C_2 Y_o(\xi r) \tag{4}$$

$$A_{2z} = C_3 H_o^{(1)}(\varphi r) \tag{5}$$

where

$$\xi = \sqrt{k_1^2 - k^2} \qquad \varphi = \sqrt{k_o^2 - k^2} \tag{6}$$

J_o, Y_o are Bessel functions of the first and second kinds and zero order, $H_o^{(1)}$ is the Hankel function of the first kind and zero order, C_1, C_2, C_3 are arbitrary constants to be determined from the boundary conditions.

All transformed field components can be expressed in terms of $\bar{A}_z$. They are

$$\bar{E}_{1\theta} = \bar{B}_{1r} = \bar{B}_{1z} = \bar{E}_{2\theta} = \bar{B}_{2r} = \bar{B}_{2z} = 0 \tag{7}$$

$$\bar{E}_{1z} = \frac{i\omega\xi^2}{k_1^2} \bar{A}_{1z} \tag{8}$$

$$\bar{E}_{2z} = \frac{i\omega\varphi^2}{k_o^2} \bar{A}_{2z} \tag{9}$$

$$\bar{E}_{1r} = -\frac{\omega k}{k_1^2} \frac{\partial \bar{A}_{1z}}{\partial r} \tag{10}$$

$$\bar{E}_{2r} = -\frac{\omega k}{k_o^2} \frac{\partial \bar{A}_{2z}}{\partial r} \tag{11}$$

$$\bar{B}_{1\theta} = -\frac{\partial \bar{A}_{1z}}{\partial r} \tag{12}$$

$$\bar{B}_{2\theta} = -\frac{\partial \bar{A}_{2z}}{\partial r} \tag{13}$$

By applying the following boundary conditions:

(a) Tangential $\overline{E}$-field continuous at $r = b$

(b) Tangential $\overline{B}$-field continuous at $r = b$

(c) Tangential $\overline{E}$-field at $r = a$, $\overline{E}_{1z}(r = a) = -V$ which is the Fourier transform of $-v\delta(z)$ and by the use of the Wronskian of Y_o and J_o, the constants are determined. They are given by

$$C_1 = -\frac{Vk_1^2}{i\omega\xi^2 D(k)} [\xi H_1^{(1)}(\varphi b) Y_o(\xi b) - \epsilon_r \varphi H_o^{(1)}(\varphi b) Y_1(\xi b)] \tag{14}$$

$$C_2 = \frac{Vk_1^2}{i\omega\xi^2 D(k)} [\xi H_1^{(1)}(\varphi b) J_o(\xi b) - \epsilon_r \varphi H_o^{(1)}(\varphi b) J_1(\xi b)] \tag{15}$$

$$C_3 = -\frac{2k_1^2 V}{i\omega\pi b\xi\varphi D(k)} \tag{16}$$

where

$$D(k) = \{\xi H_1^{(1)}(\varphi b) [J_o(\xi a) Y_o(\xi b) - J_o(\xi b) Y_o(\xi a)] - \epsilon_r \varphi H_o^{(1)}(\varphi r) [J_o(\xi a) Y_1(\xi b) - J_1(\xi b) Y_o(\xi a)]\} \tag{17}$$

The next step is the substitution of (14), (15), (16), and (17) together with (4) and (5) into (7) to (13). The transformed field quantities can now be written explicitely as follows:

$$\bar{E}_{1z} = -\frac{V}{D(k)}\{\xi H_1^{(1)}(\varphi b)[Y_o(\xi b)J_o(\xi r) - J_o(\xi b)Y_o(\xi r)] - \epsilon_r \varphi H_o^{(1)}(\varphi b)[Y_1(\xi b)J_o(\xi r) - J_1(\xi b)Y_o(\xi r)]\} \quad (18)$$

$$\bar{E}_{2z} = -\frac{2\epsilon_r \varphi V}{\pi b \xi D(k)} H_o^{(1)}(\varphi r) \quad (19)$$

$$\bar{E}_{1r} = -\frac{kV}{-i\xi D(k)}\{\xi H_1^{(1)}(\varphi b)[Y_o(\xi b)J_1(\xi r) - J_o(\xi b)Y_1(\xi r)] - \epsilon_r \varphi H_o^{(1)}(\varphi b)[Y_1(\xi b)J_1(\xi r) - J_1(\xi b)Y_1(\xi r)]\} \quad (20)$$

$$\bar{E}_{2r} = -\frac{2\epsilon_r kV}{i\pi b \xi D(k)} H_1^{(1)}(\varphi r) \quad (21)$$

$$\bar{B}_{1\theta} = -\frac{k_1^2 V}{i\omega \xi D(k)}\{\xi H_1^{(1)}(\varphi b)[Y_o(\xi b)J_1(\xi r) - J_o(\xi b)Y_1(\xi r)] - \epsilon_r \varphi H_o^{(1)}(\varphi b)[Y_1(\xi b)J_1(\xi r) - J_1(\xi b)Y_1(\xi r)]\} \quad (22)$$

$$\bar{B}_{2\theta} = -\frac{2k_1^2 V}{i\omega\pi b \xi D(k)} H_1^{(1)}(\varphi r) \quad (23)$$

By inversion of the Fourier transform the actual field quantities can be calculated according to (3-b). The singularities and path of integration will be discussed in the next part. It is noted that by this approach the vector potential is discontinuous at $r = b$. Therefore, fields exist at

$r = b$ only in the limit sense, as $r \to b$, either from the outside or from the inside. An alternative procedure is to solve the wave equation for E_z directly. The solutions are precisely the same.

B. Current Distribution

The transformed current in the antenna can be found from the application of the fourth boundary condition—which has not been used so far. It concerns the tangential $\overline{B}$-field at $r = a$. If the antenna is assumed to be a perfect conductor, it is

$$\overline{I}(k) = \frac{2\pi a}{\mu_o} \overline{B}_{1\theta}(r = a) \tag{24}$$

With the substitution of $\overline{B}_{1\theta}$ from (22) with $r = a$ and the inversion of the Fourier transform according to (3-b), the current distribution as a function of z is found to be

$$I(z) = ia\omega\epsilon_1 V \int_c \frac{dk e^{-ikz}}{\xi D(k)} \{\xi H_1^{(1)}(\varphi b)[Y_o(\xi b)J_1(\xi a) - J_o(\xi b)Y_1(\xi a)] - \epsilon_r \varphi H_o^{(1)}(\varphi b)[Y_1(\xi b)J_1(\xi a) - J_1(\xi b)Y_1(\xi a)]\} \tag{25}$$

The contour of integration, the branch cuts, and the principal Riemann sheet are defined in Figure 2. The contour of integration is defined to satisfy the radiation condition, and the branch cut is drawn so that the path of integration can be deformed and easily computed.

Before carrying out any calculation, the singularities of the integrand must be investigated. Note that the points $k = \pm k_1$ are not branch points. This can be verified easily by adding π to the argument of $\xi = \sqrt{k_1^2 - k^2}$ the integrand is unchanged. The only branch points left are at $k = \pm k_o$. Poles can be determined from the equation $D(k) = 0$, which will be discussed step by step as follows:

(a) On the real axis $k_1 < |k| < \infty$, define

$$\alpha = \sqrt{k^2 - k_1^2} = -i\xi \quad ; \quad \beta = \sqrt{k^2 - k_o^2} = -i\varphi \tag{26}$$

which are real and positive. Equation (17) can be rewritten as

$$D(k) = \frac{4}{\pi}\{\alpha K_1(\beta b)[I_o(\alpha b)K_o(\alpha a) - I_o(\alpha a)K_o(\alpha b)] + \beta \epsilon_r K_o(\beta b)[I_1(\alpha b)K_o(\alpha a) + I_o(\alpha a)K_1(\alpha b)]\} \tag{27}$$

where K_o, I_o and K_1, I_1 are modified Hankel and Bessel functions of zero and first order. For real and positive α and β, K_o, I_o, K_1, I_1 are all real and positive. Moreover, $I_o(\alpha b) > I_o(\alpha a)$, $K_o(\alpha a) > K_o(\alpha b)$ so that $D(k)$ is always greater than zero. No pole exists on this part of the real axis.

(b) On the real axis $k_o < |k| < k_1$, the equation $D(k) = 0$ becomes

$$\xi K_1(\beta b)[J_o(\xi a)Y_o(\xi b) - J_o(\xi b)Y_o(\xi a)] + \epsilon_r \beta K_o(\beta b)[J_o(\xi a)Y_1(\xi b) - J_1(\xi b)Y_o(\xi a)] = 0 \tag{28}$$

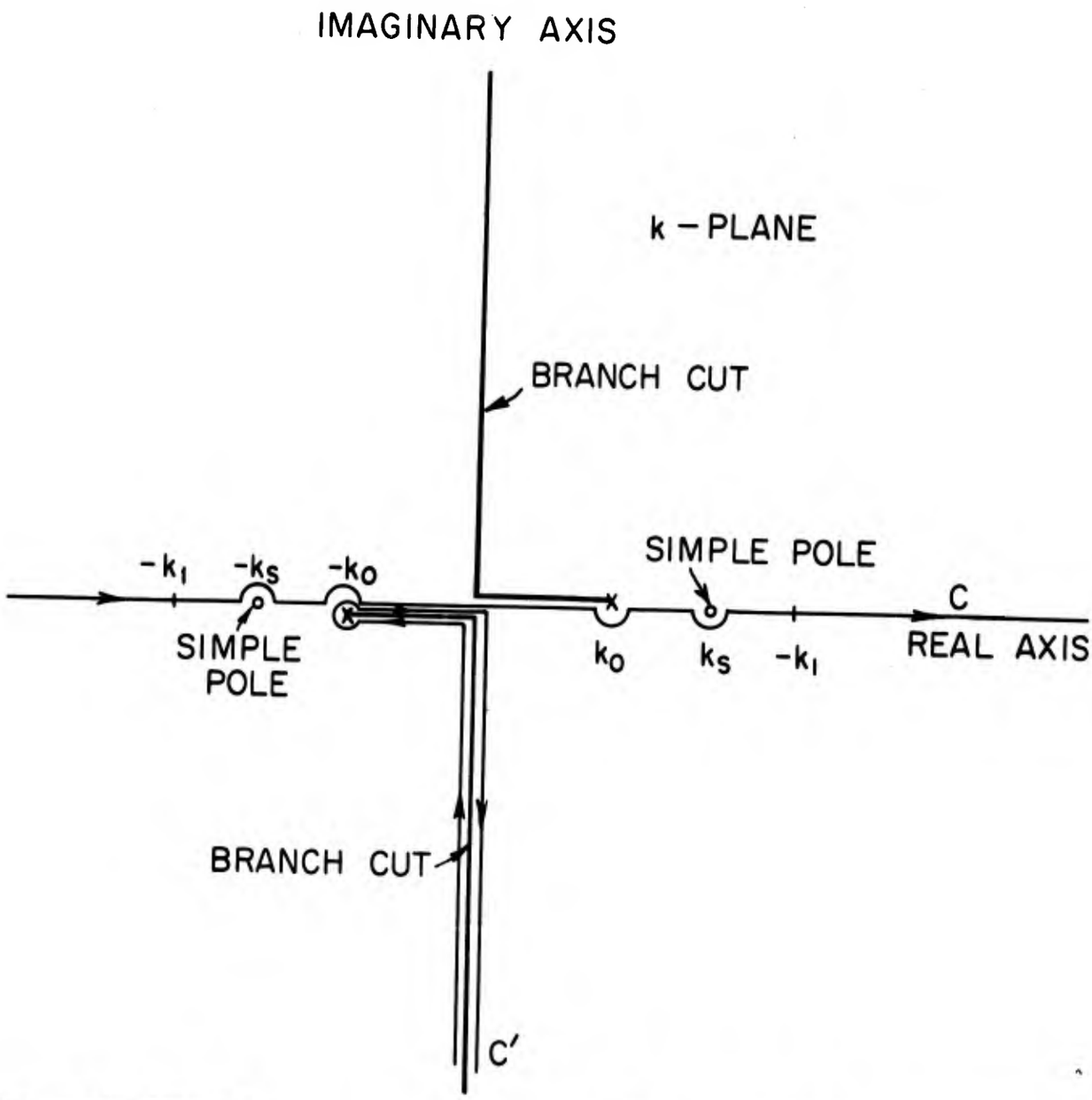

$$\sqrt{k_o^2-k^2} = i\sqrt{k^2-k_1^2}$$

$$-\frac{\pi}{2} < \mathrm{Arg}\sqrt{k^2-k^2} < \frac{\pi}{2}$$

$$\sqrt{k^2-k_o^2} \to k \quad \text{AS} \quad k \to \infty$$

FIG. 2 INTEGRATION PATHS C, C′ AND SINGULARITIES ON k – PLANE

which is just the characteristic equation of a Goubau transmission line [3], [4]. It can be shown by plotting (28) that for $\epsilon_r = 3.00$, $k_o a = 0.04$, b/a up to 8 that only the lowest fundamental mode (or E_{oo} mode) exists. This is called the Goubau surface-wave mode. It has no cutoff. Its wave number is designated by k_s. Figure 3 shows the curve k_s/k_o as a function of the thickness b/a when $\epsilon_r = 3.00$, $k_o a = 0.04$.

(c) On the real axis $0 < |k| < k_o$, and on the entire imaginary axis, if there is a pole which makes $D(k) = 0$, then

$$\frac{\xi[J_o(\xi a)Y_o(\xi b) - J_o(\xi b)Y_o(\xi a)]}{\epsilon_r \varphi[J_o(\xi a)Y_1(\xi b) - J_1(\xi b)Y_o(\xi a)]} = \frac{H_o^{(1)}(\varphi b)}{H_1^{(1)}(\varphi b)} \tag{29}$$

The left-hand side is always real (on either side of the branch cut). The right-hand side is in general complex and equal to $\dfrac{J_o(\varphi b) + iY_o(\varphi b)}{J_1(\varphi b) + iY_1(\varphi b)}$. For the right-hand side to be real it is necessary that

$$\frac{J_o(\varphi b)}{J_1(\varphi b)} = \frac{Y_o(\varphi b)}{Y_1(\varphi b)} \tag{30}$$

It follows from the Wronskian of J_o and Y_o, that this equality can never be satisfied except at infinity and at $k = \pm k_o$—which will be discussed later. Consequently, there is no pole on either side of the branch cuts.

(d) For very large values of $|k|$, the asymptotic form of the Bessel functions can be used. It can be shown that $D(k)$ behaves like

$$D(k) \sim \frac{2\sqrt{2}\, e^{i(\varphi b - \frac{\pi}{4})}}{\pi \xi \sqrt{ab\pi\varphi}} \{-i\xi \sin[\xi(b-a)] + \epsilon_r \varphi \cos[\xi(b-a)]\} \quad (31)$$

which has an essential zero at infinity. In the finite domain of large $|k|$, the existence of a pole, or a zero of $D(k)$, requires that

$$\tan[\xi(b-a)] = -i\frac{\varphi}{\xi}\epsilon_r \approx \mp i\epsilon_r \quad (32-a)$$

$$\text{or} \quad \tanh[\alpha(b-a)] \approx \mp \epsilon_r \quad (32-b)$$

$$\text{or} \quad \alpha(b-a) \approx \frac{1}{2} \ln \frac{1 \mp \epsilon_r}{1 \pm \epsilon_r} + in\pi \quad (32-c)$$

where the upper sign is for $-\frac{\pi}{2} < \arg \alpha < \frac{\pi}{2}$, and the lower sign is for $\frac{\pi}{2} < \arg \alpha < \frac{3\pi}{2}$; n is a very large integer. In either case, (32-c) breaks down owing to the different algebraic signs of the real parts on the two sides. Furthermore, the zero at infinity is just canceled out by the zero in the numerator at infinity, so that the whole integrand behaves like

$$\sim \frac{-i\xi \cos[\xi(b-a)] - \epsilon_r \varphi \sin[\xi(b-a)]}{\xi\{-i\xi \sin[\xi(b-a)] + \epsilon_r \varphi \cos[\xi(b-a)]\}}$$

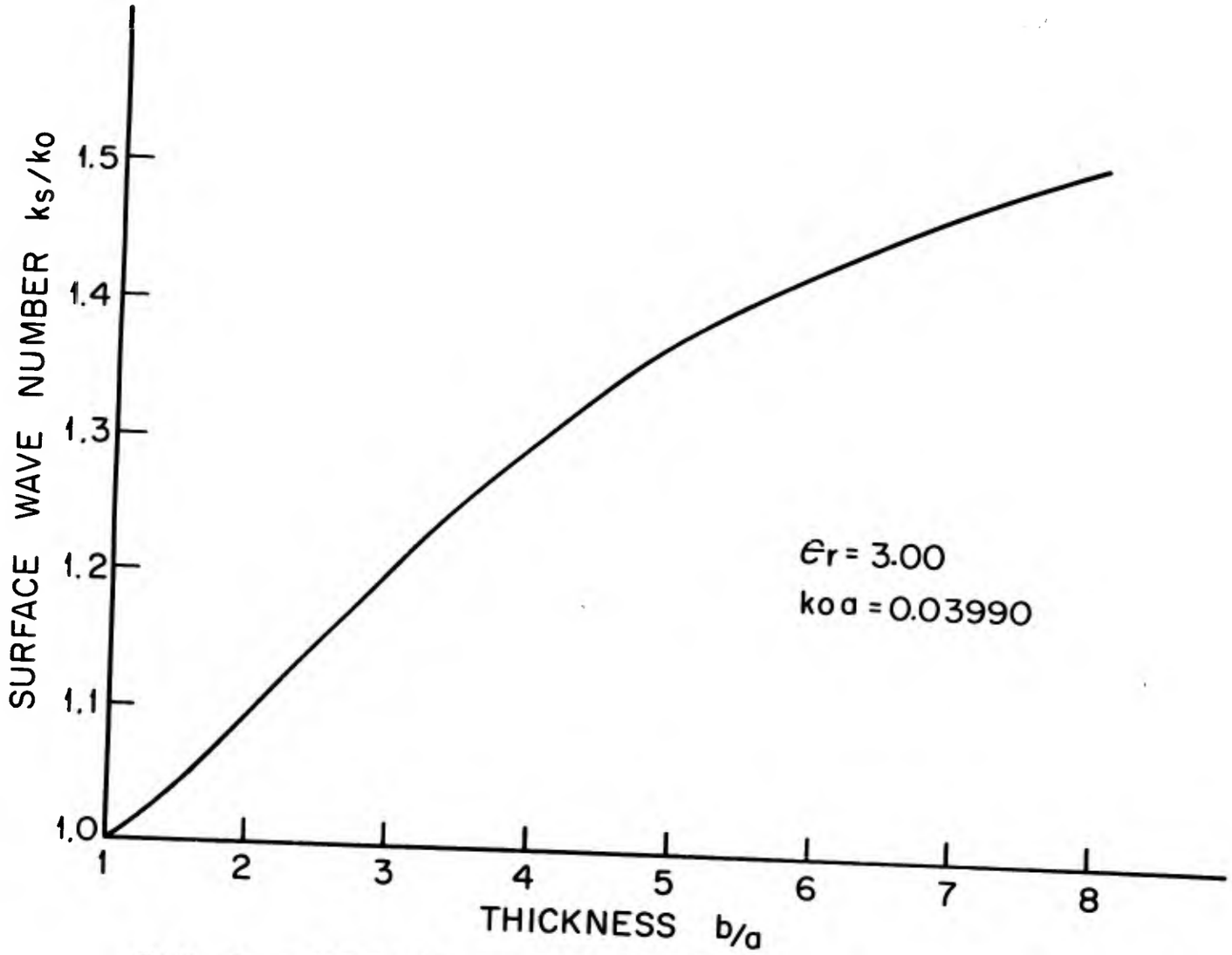

FIG. 3 SURFACE WAVE NUMBER k_s/k_o AS FUNCTION OF THICKNESS

which is always finite on the principal sheet. Therefore, the conclusion is reached that there is no pole in the domain of very large $|k|$ including infinity.

(e) In the finite complex plane, the poles are very difficult to locate. From the above knowledge, and from the limit behavior of the integrand as $k_1 \to k_o$, it can be shown that there is no pole in the finite complex plane. As $k_1 \to k_o$, D(k) approaches $\frac{2}{\pi\varphi b} H_o^{(1)}(\varphi a)$, which has no zero anywhere except at infinity; therefore, if D(k) has a zero somewhere on the principal sheet of the finite complex plane it must go somewhere else in the limit as $k_1 \to k_o$. However, since it can neither cross the branch cut and go into the other Riemann sheet by (c), nor go to infinity by (d) (since it must cross the region of large $|k|$) the only possible path for this zero if it is to vanish is to go through k_o. Now, the problem is to show that in the vicinity of k_o, there can be no pole except k_s during the process $k_1 \to k_o$. The existence of a pole requires that

$$\frac{\varphi H_o(\varphi b)}{H_1(\varphi b)} = \frac{\xi \left[J_o(\xi a) Y_o(\xi b) - J_o(\xi b) Y_o(\xi a)\right]}{\epsilon_r \left[J_o(\xi a) Y_1(\xi b) - J_1(\xi b) Y_o(\xi a)\right]} \tag{33}$$

In the vicinity of k_o, let $k = k_o + \delta e^{i\theta}$, where δ can be made arbitrarily small and $-\pi < \theta < \pi$. Let the left-hand side of (33) be expanded for small arguments of the Bessel functions. Thus,

$$H_1^{(1)}(\varphi b) \approx -\frac{2}{\pi b\sqrt{2k_o}\,\delta^{1/2} e^{i\theta/2}} \tag{34}$$

$$\varphi H_o^{(1)}(\varphi b) \approx -\sqrt{2k_o}\,\delta^{1/2}\, e^{i\theta/2}\,\frac{2}{\pi}\left[\ell n\,\frac{b\sqrt{2k_o\delta}}{2} + i\frac{\theta}{2} + \gamma\right] \tag{35}$$

where γ is Euler's constant. Let the right-hand side of (33) be expanded in a Taylor's series. The resulting equation is

$$2bk_o\delta\, e^{i\theta}\left[\ell n\,\frac{b\sqrt{2k_o\delta}}{2} + i\frac{\theta}{2} + \gamma\right] = A + \delta\, e^{i\theta} B \tag{36}$$

where A is equal to the right-hand side of (33) with k replaced by k_o and B is equal to the derivative of the right-hand side of (33) with respect to k and then with k_o substituted for k. Both A and B are constants independent of δ. If the real and the imaginary parts of (19) are equated, the result is

$$2bk_o\delta\left[\ell n\,\frac{b\sqrt{2k_o\delta}}{2} + \gamma\right] = A\cos\theta + \delta B \tag{37}$$

$$bk_o\delta\,\theta = -A\sin\theta \tag{38}$$

In (37), δ can certainly be sufficiently small so that both γ and B are negligible compared with the logarithmic term. If they are omitted and (38) is divided by (37) the following final formula is obtained:

$$\tan\theta = \frac{-\theta}{2\,\ell n\left(\frac{b\sqrt{2k_o\delta}}{2}\right)} \tag{39}$$

For very small δ, (21) is true only at $\theta = 0$, that is on the real axis. But the behavior of D(k) on the real axis is well-known: there can be no pole other than k_s. It follows that the whole complex plane has been studied, that the only singularities on the principal sheet are the branch cuts drawn from the branch points at $\pm k$ and two simple poles at $\pm k_s$.

In the evaluation of the integral (25) for the current, the contour of integration C can be closed in the lower half plane for positive z, since there is no contribution due to the big circle at infinity. As shown in Figure 2, the contribution from the simple pole at $-k_s$, which is called the surface-wave current or the transmission current and is designated by $I_s(z)$, is

$$I_s(z) = \left[-\frac{4a\omega\epsilon_1 V e^{-ikz}}{\xi \frac{d}{dk} D(k)} \{ \xi K_1(\beta b)[Y_o(\xi b)J_1(\xi a) - J_o(\xi b)Y_1(\xi a)] + \epsilon_r \beta K_o(\beta b)[Y_1(\xi b)J_1(\xi a) - J_1(\xi b)Y_1(\xi a)] \} \right]_{k=-k_s} \tag{40}$$

Equation (40) shows that the transmission current has a constant amplitude and a real and finite value at $z = 0$.

The contribution due to the branch-cut integration C', which is called radiation current and designated by $I_r(z)$, can be expressed as follows:

$$I_r(z) = \frac{16\omega\epsilon_1\epsilon_r V}{\pi^3 b^2} \int_o^{k_o} \frac{e^{ixz}\,dx}{(k_1^2 - x^2)\{[A(\sqrt{k_1^2-x^2}, \sqrt{k_o^2-x^2})]^2 + [B(\sqrt{k_1^2-x^2}, \sqrt{k_o^2-x^2})]^2\}}$$

$$-i\int_o^{\infty} \frac{e^{-yz}\,dy}{(k_1^2+y^2)\{[A(\sqrt{k_1^2+y^2}, \sqrt{k_o^2+y^2})]^2 + [B(\sqrt{k_1^2+y^2}, \sqrt{k_o^2+y^2})]^2\}} \tag{41}$$

where

$$A(p, q) = pJ_1(qb)[Y_o(pb)J_o(pa) - J_o(pb)Y_o(pa)]$$

$$- \epsilon_r q J_o(qb)[J_o(pa)Y_1(pb) - J_1(pb)Y_o(pa)] \tag{42-a}$$

$$B(p, q) = pY_1(qb)[Y_o(pb)J_o(pa) - J_o(pb)Y_o(pa)]$$

$$- \epsilon_r q Y_o(qb)[J_o(pa)Y_1(pb) - J_1(pb)Y_o(pa)] \tag{42-b}$$

Equation (41) shows that the real part of the radiation current is finite, and the imaginary part infinite at $z = 0$. These are the same properties which characterize an infinite cylindrical antenna in free space [5]. Both transmission current and radiation current have been computed. These are shown graphically in Figure 4 for $\epsilon_r = 3.0$, $k_o a = 0.04$; and b/a varies from 1.1 to 8.

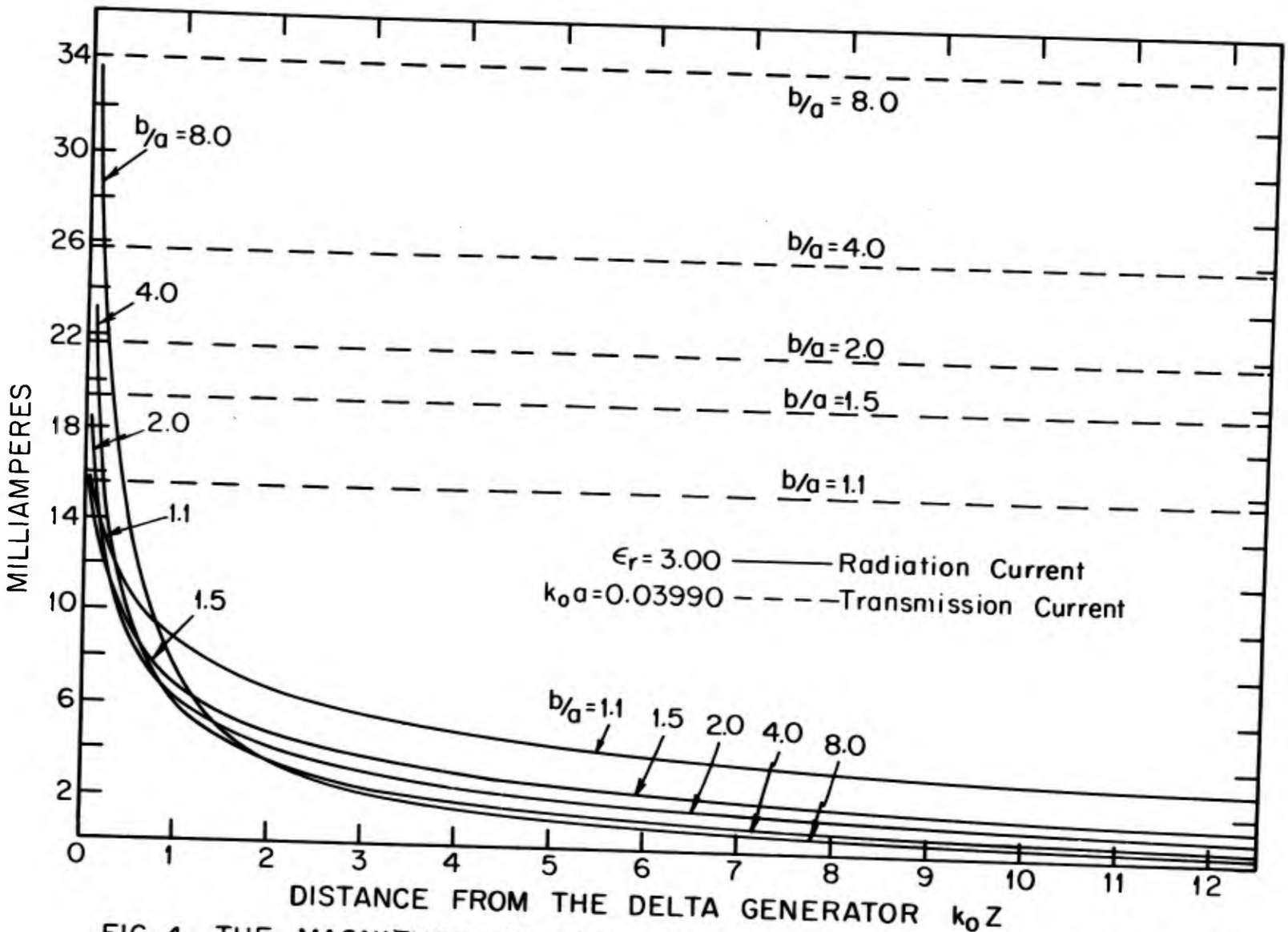

FIG. 4 THE MAGNITUDE OF RADIATION AND TRANSMISSION CURRENTS ALONG INFINITE CYLINDRICAL DIELECTRIC COATED ANTENNAS.

C. Asymptotic Behavior of the Current at Infinity and Near the Driving Point

The graphs in Figure 4 indicate that the radiation current decays very rapidly along the line, while the transmission current is constant. As $z\to\infty$ the asymptotic expansion of the radiation current can be found by the successive integration by parts of (41). The leading term is obtained after two integrations. It is

$$I_r(z\to\infty) \sim \frac{-8\,k_o\omega\epsilon_o\epsilon_r^2 V e^{ik_o z}}{\pi z^2\{(k_1^2-k_o^2)[Y_o(\sqrt{k_1^2-k_o^2}\,b)J_o(\sqrt{k_1^2-k_o^2}\,a) - J_o(\sqrt{k_1^2-k_o^2}\,b)Y_o(\sqrt{k_1^2-k_o^2}\,a)]\}^2} \tag{43}$$

This differs from the current along an infinite cylindrical antenna in free space whose asymptotic current distribution is essentially constant or decays slowly as $1/\ell n\, z$. The asymptotic behavior of the current at infinity for an infinite dielectric-coated antenna is $1/z^2$. The current very close to the driving point is determined by the asymptotic form of (24) as $k\to\infty$, which is

$$\overline{I}(k\to\infty) \sim \frac{-i2\pi a\omega\epsilon_1 V}{|k|} \tag{44}$$

From an inspection of the table of cosine transforms, it is seen that $I(z\to 0)$ should behave as

$$I(z\to 0) \sim -i4a\omega\epsilon_1 V\,\ell n\, z \tag{45}$$

It is very similar to the free-space case [6] in that both have a logarithmic singularity at the driving point. It differs from the free-space case only by a factor ϵ_r. Another interesting fact is that the current very close to the driving point as given by (45) is independent of the radius of the dielectric cylinder b, and is the same as in an infinite dielectric medium.

D. Radiation Pattern

The magnetic field in region II is obtained by inverting $\bar{B}_{2\theta}$ in (23). The result is

$$\bar{B}_{2\theta} = \frac{-k_1^2 V}{i\omega\pi^2 b} \int_c \frac{H_1^{(1)}(\varphi r)}{\varepsilon D(k)} e^{-ikz}\, dk \tag{46}$$

where the path of integration is the same as defined in Figure 2. After a change to the spherical coordinated (R, θ, ϕ) with

$$z = R\cos\theta \quad , \quad r = R\sin\theta \tag{47}$$

let $R\to\infty$. It then follows from (46) that

$$B_{2\theta}(R\to\infty) \sim \frac{k_1^2 V e^{-i\frac{\pi}{4}}}{\omega\pi^2 b}\sqrt{\frac{2}{\pi R\sin\theta}} \int_c \frac{e^{iR(\varphi\sin\theta - k\cos\theta)}}{\sqrt{\varphi}\,\varepsilon D(k)}\, dk \tag{48}$$

An application of the method of steepest descents and the evaluation of the integral at saddle point $k = -k_o \cos\textcircled{H}$, yields the asymptotic form of $B_{2\theta}$ as $R \to \infty$. It is

$$B_{2\theta}\,(R\to\infty) \sim \frac{2k_1^2 V}{\omega\pi^2 b}\left[\frac{1}{\xi D(k)}\right]_{k=-k_o\cos\theta} \frac{e^{ik_o R}}{R} \tag{49}$$

The Poynting vector in the far field is, by definition,

$$S = \frac{1}{2\mu_o} E_2 X B_2^* = \frac{1}{2\mu_o\sqrt{\mu_o\epsilon_o}} |B_{2\theta}|^2$$

$$= \frac{2k_1^2\epsilon_r V^2}{\pi^4 R^2 b^2}\sqrt{\frac{\epsilon_o}{\mu_o}} \left|\frac{1}{\xi D(k)}\right|^2_{k=-k_o\cos\theta} \tag{50}$$

Let the radiation factor be defined as follows:

$$R_r(\textcircled{H}) = 4\pi R^2 S = \frac{k_o^2\epsilon_r^2 V^2}{15\pi^4 b^2} \left|\frac{1}{\xi D(k)}\right|^2_{k=-k_o\cos\textcircled{H}} \tag{51}$$

Equation (51) has been computed and represented graphically in Figure 5. The radiation factor is zero at $\theta = 0$. This agrees with the $1/z^2$ asymptotic behavior of the current. The far field should decay as $1/R$. If the field decays faster than $1/R$ in certain directions, the radiation pattern must have a zero in that direction. On the other hand, if the field decays slower than $1/R$, then the radiation pattern should be

infinite in that direction as in the case of an infinite cylindrical antenna in free space at $\textcircled{H} = 0$ [9].

E. Transmission Admittance and Transmitted Power

The transmission admittance Y_s due to the surface-wave mode is defined to be $\lim_{z \to 0} \frac{I_z^s(z)}{V}$. With the help of (40), it is found to be

$$Y_s = \left[\frac{-4a\omega\epsilon_1}{\xi \frac{d}{dk} D(k)} \{ \xi K_1(\beta b)[Y_o(\xi b)J_1(\xi a) - J_o(\xi b)Y_1(\xi a)] + \epsilon_r \beta K_o(\beta b)[Y_1(\xi b)J_1(\xi a) - J_1(\xi b)Y_1(\xi a)] \} \right]_{k=-k_s} \tag{52}$$

Equation (52) shows that the transmission impedance is a real quantity. Note that $Y_s = G_s$ is the transmission conductance. The transmitted power is

$$P_s = \frac{1}{2} V^2 G_s \tag{53}$$

The same answer is obtained if the normal component of the part of the Poynting vector associated with the surface-wave mode is integrated over two infinite surfaces perpendicular to the antenna at $+z$ and $-z$ respectively. This is shown in Appendix 1.

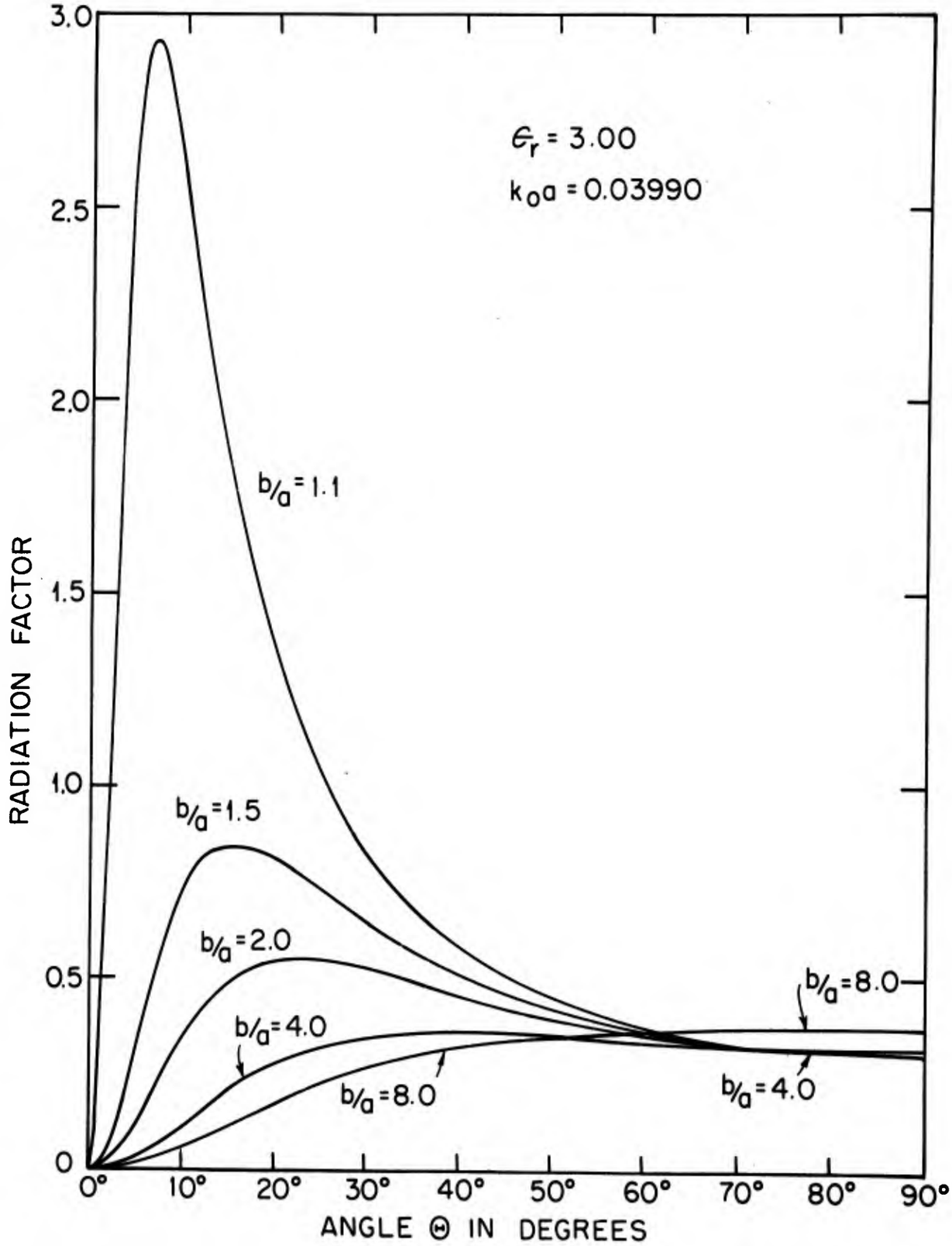

FIG. 5 RADIATION PATTERNS OF DIELECTRIC COATED INFINITE CYLINDRICAL ANTENNAS

F. Radiation Conductance and Radiated Power

The radiation conductance G_r is defined as follows:

$$\lim_{z \to 0} \left[\mathrm{Re} \left(\frac{I_z^R(z)}{V} \right) \right].$$

With (22), it is

$$G_r = \frac{16 \omega \epsilon_1 \epsilon_r}{\pi^3 b^2} \int_o^{k_o} \frac{dx}{(k_1^2 - x^2)\{A(\sqrt{k_1^2 - x^2}, \sqrt{k_o^2 - x^2})]^2 + [B(\sqrt{k_1^2 - x^2}, \sqrt{k_o^2 - x^2})]^2\}} \tag{54}$$

where $A(p, q)$ and $B(p, q)$ are defined in (42-a) and (42-b). The radiated power can be calculated immediately from

$$P_r = \frac{1}{2} V^2 G_r \tag{55}$$

Again, the integration of the normal component of the Poynting vector (50) over a very large sphere yields the same answer. This is shown in Appendix 2.

The total input conductance is, therefore, $G_{in} = G_s + G_r$. G_s, G_r, and G_{in} are shown in Figure 6 as functions of b/a with $\epsilon_r = 3.00$, $k_o a = 0.04$. The efficiency of transmission E_s and the radiating efficiency E_r are defined as follows:

$$E_s = \frac{P_s}{P_s + P_r} = \frac{G_s}{G_{in}} \tag{56}$$

$$E_r = \frac{P_r}{P_s + P_r} = \frac{G_r}{G_{in}} \tag{57}$$

These quantities are shown graphically in Figure 7 as a function of b/a.

G. Conclusions

The above analysis and the results obtained suggest that a comparison with an infinite cylindrical antenna in free space is of interest. Note that the latter can always be considered to be a limiting case of a dielectric-coated antenna as $b/a \to 1$. Important differences can be summarized as follows:

(a) For a dielectric coated infinite cylindrical antenna a T.M. surface wave or Goubau wave is excited. Therefore, there are two kinds of current in the antenna; the one called transmission current and the other called radiation current. It is noted, from the results shown in Figure 4, that the radiation current decreases while the transmission current increases as the dielectric coating gets thicker. In the limiting case, as the thickness of the coating tends to zero, only the radiation current remains. This is just the case of the infinite cylindrical antenna in free space. It is also noted, that as the coating gets thicker, the transmission current immediately becomes the dominant part. When $b/a = 8$, the radiation current is very small and

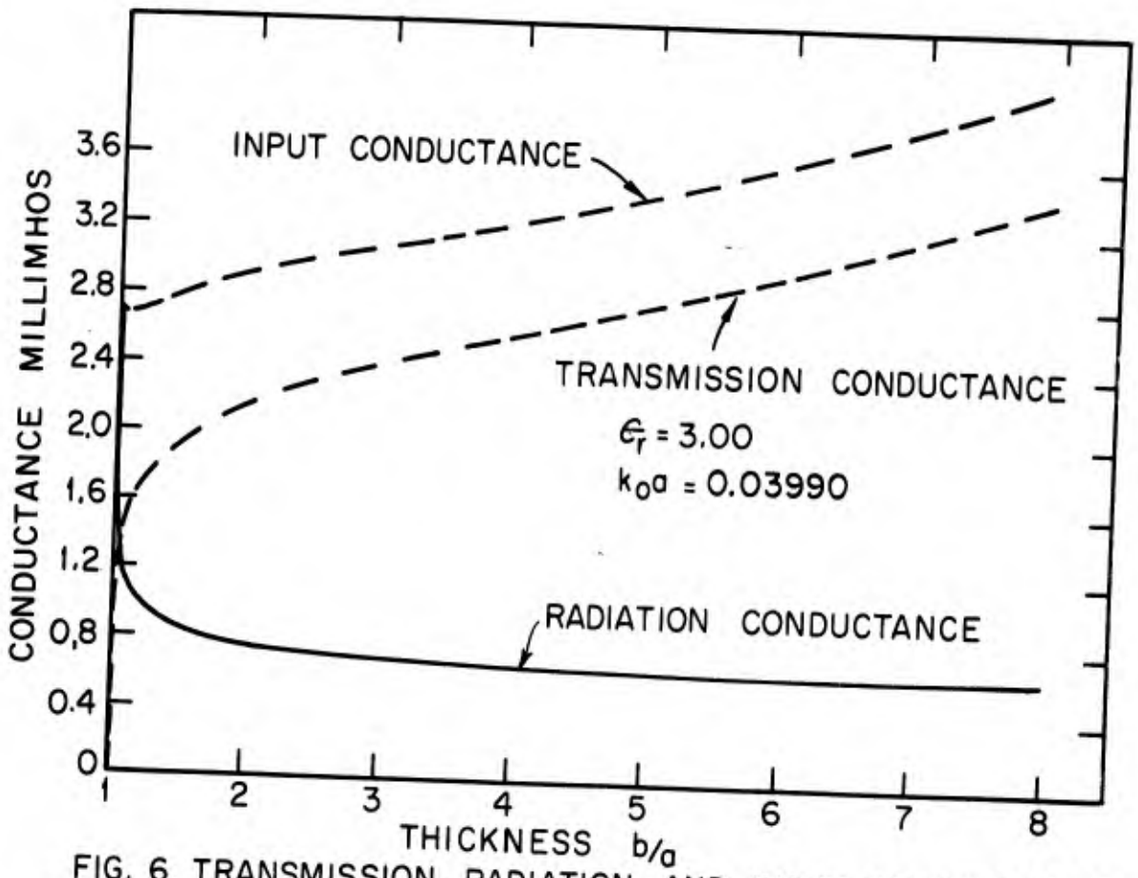

FIG. 6 TRANSMISSION, RADIATION AND INPUT CONDUCTANCES

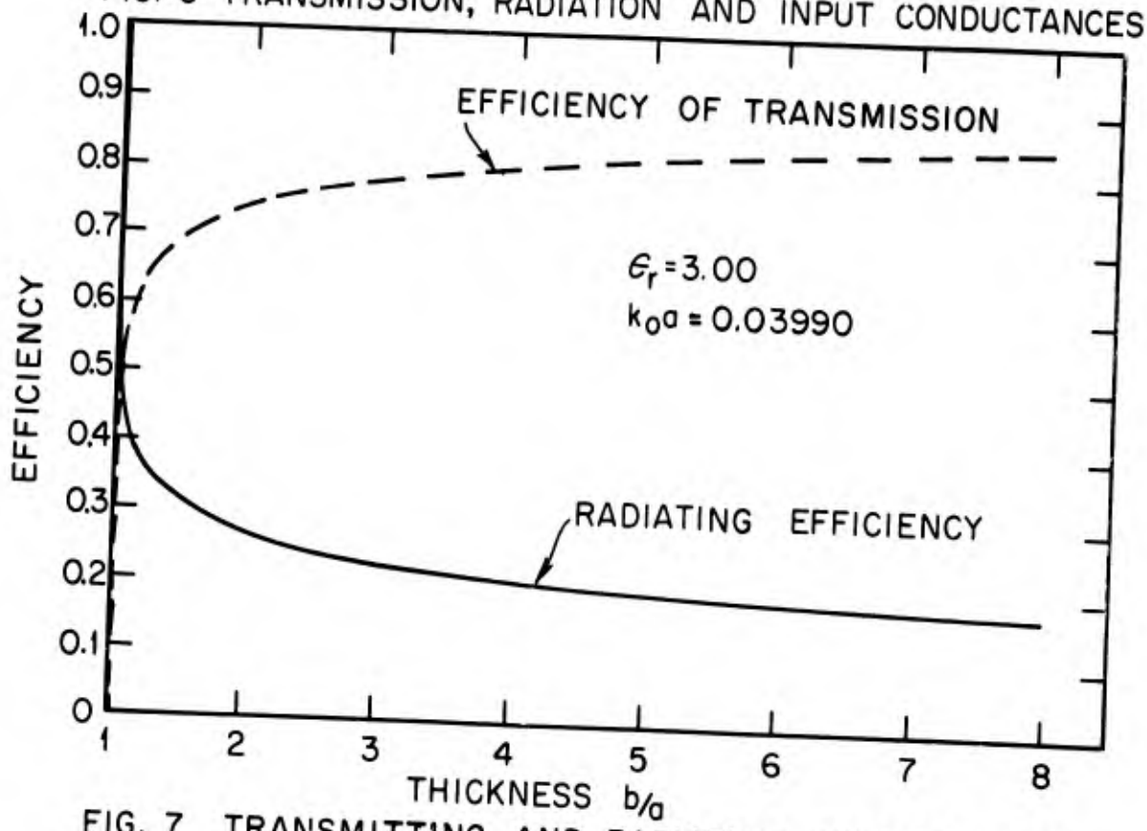

FIG. 7 TRANSMITTING AND RADIATING EFFICIENCIES

can certainly be neglected compared with the transmission current except very close to the delta generator, where theoretically the radiation current is unbounded.

(b) The asymptotic forms of the radiation current as $z \to \pm\infty$ are different in the two cases. For a dielectric-coated antenna it behaves as $1/z^2$, whereas for a noncoated one, it is essentially constant or $1/\ell n\, z$.

(c) Associated with those two kinds of current are two kinds of power flow for a dielectric-coated antenna. The transmitted power flows toward $\pm z$ directions, and the radiated power is transferred to all of space. The former increases and the latter decreases as the coating gets thicker. In the limiting case b/a=1 the transmitted power vanishes.

(d) The radiated pattern changes greatly with b/a. Figure 5 shows that the antenna has end-fire characteristics at first with b/a very small, but gradually acquires a broadside behavior as b/a increases With the uncoated antenna, the radiation pattern goes to infinity at $\theta=0$ as can be predicted from the results in Figure 5.

(e) From the properties discussed before, predictions can be made for a finite antenna in a dielectric rod. Since for a rather thick dielectric-coated infinite cylindrical antenna the dominant current is transmitted along the cylinder with the propagation constant k_s rather than radiated with the propagation constant k_o, it may be anticipated that the current in a finite coated antenna, instead of being

approximated by a sine and a shifted cosine term with the propagation constant k_o, should be represented by a sine and a shifted cosine term with the propagation constant k_s.

III. THE FINITE CYLINDRICAL DIELECTRIC-COATED ANTENNA

A. Formulation of the Integral Equation

One way to formulate the integral equation for the current in a finite antenna is to derive the Green's function first. Suppose there is a ring delta-function current source with radius a, oriented in the z-direction inside a concentric dielectric rod with radius b as shown in Figure 8(a). Rotational symmetry still holds, and only the z-component of the vector potential, $\vec{G} = G\hat{z}$, is excited. The vector potential G in the dielectric medium and in free space due to this delta function source satisfies the following wave equations.

$$\frac{1}{r}\frac{\partial}{\partial r}\left(r\frac{\partial G}{\partial r}\right) + \frac{\partial^2 G}{\partial z^2} + k_1^2 G = -\frac{\mu_o}{2\pi r}\delta(z)\,\delta(r-a) \qquad 0 < r < b \tag{1}$$

$$\frac{1}{r}\frac{\partial}{\partial r}\left(r\frac{\partial G}{\partial r}\right) + \frac{\partial^2 G}{\partial z^2} + k_o^2 G = 0 \qquad b < r < \infty \tag{2}$$

where a factor $\frac{1}{2\pi r}$ is used to make the total current equal to unity. By the method used in Section II, the Fourier-transformed vector potential $\bar{G}(k, r)$ in each region can be obtained. It is given by

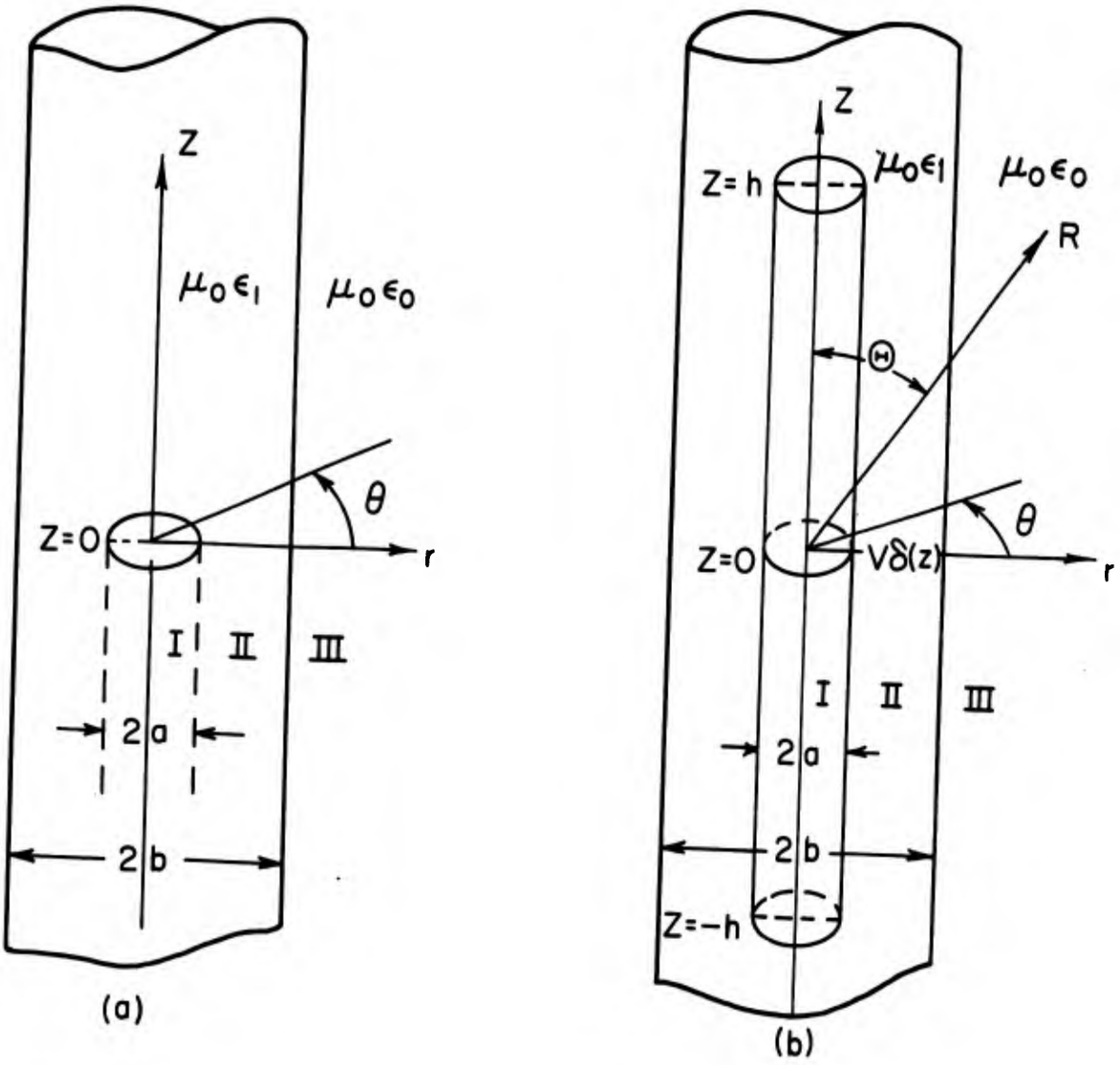

FIG. 8 SCHEMATIC DIAGRAMS OF A RING DELTA SOURCE (a) AND A FINITE DIPOLE (b) IN A INFINITE DIELECTRIC ROD.

$$\bar{G}_1(k, r) = C_1 J_o(\xi r) \qquad 0 < r \leq a \tag{3}$$

$$\bar{G}_2(k, r) = C_2 J_o(\xi r) + C_3 Y_o(\xi r) \qquad a < r < b \tag{4}$$

$$\bar{G}_3(k, r) = C_4 H_o(\varphi r) \qquad b < r < \infty \tag{5}$$

where $\xi = \sqrt{k_1^2 - k^2}$, $\varphi = \sqrt{k_o^2 - k^2}$ is defined in the same manner as before. The boundary conditions in this case are:

(a) Tangential electric field continuous at $r = a$,

$$\bar{G}_1(k, a) = \bar{G}_2(k, a) \tag{6}$$

(b) Tangential magnetic field discontinuous at $r = a$. The integration of (1) from $a - \delta$ to $a + \delta$, where δ is a very small positive quantity, gives

$$\frac{\partial \bar{G}_1(k, a)}{\partial r} - \frac{\partial \bar{G}_2(k, a)}{\partial r} = \frac{\mu}{2\pi a} \tag{7}$$

(c) Tangential electric field continuous at $r = b$

$$\frac{\xi^2}{k_1^2} \bar{G}_2(k, b^-) = \frac{\varphi^2}{k_o^2} \bar{G}_3(k, b^+) \tag{8}$$

(d) Tangential magnetic field continuous at $r = b$

$$\frac{\partial \overline{G}_2(k, b^-)}{\partial r} = \frac{\partial \overline{G}_3(k, b^+)}{\partial r} \tag{9}$$

After the evaluation of C_1, C_2, C_3, and C_4 from the above four boundary conditions, the Green's function in each region may be found. In region I, $0 < r \leq a$, it is

$$\overline{G}_1(k, r) = -\frac{\mu_o J_o(\xi r)\left\{\begin{array}{l}[\epsilon_r \varphi Y_1(\xi b)H_o^{(1)}(\varphi b) - \xi Y_o(\xi b)H_1^{(1)}(\varphi b)]J_o(\xi a) \\ + [\xi J_o(\xi b)H_1^{(1)}(\varphi b) - \epsilon_r \varphi J_1(\xi b)H_o^{(1)}(\varphi b)]Y_o(\xi a)\end{array}\right\}}{4[\xi J_o(\xi b)H_1^{(1)}(\varphi b) - \epsilon_r \varphi J_1(\xi b)H_o^{(1)}(\varphi b)]} \tag{10}$$

In region II, $a \leq r < b$, it is

$$\overline{G}_2(k, r) = -\frac{\mu_o J_o(\xi a)\left\{\begin{array}{l}[\epsilon_r \varphi Y_1(\xi b)H_o^{(1)}(\varphi b) - \xi Y_o(\xi b)H_1^{(1)}(\varphi b)]J_o(\xi r) \\ + [\xi J_o(\xi b)H_1^{(1)}(\varphi b) - \epsilon_r \varphi J_1(\xi b)H_o^{(1)}(\varphi b)]Y_o(\xi r)\end{array}\right\}}{4[\xi J_o(\xi b)H_1^{(1)}(\varphi b) - \epsilon_r \varphi J_1(\xi b)H_o^{(1)}(\varphi b)]} \tag{11}$$

In region III, $b < r < \infty$, it is

$$\overline{G}_3(k, r) = \frac{\xi \mu_o \epsilon_o J_o(\xi a)H_o(\xi r)}{2\pi \varphi b[\xi J_o(\xi b)H_1^{(1)}(\varphi b) - \epsilon_r \varphi J_1(\xi b)H_o^{(1)}(\varphi b)]} \tag{12}$$

At $r = a$, either (10) or (11) can be rearranged to give

$$\bar{G}_2(k, a) = -\frac{\mu_o J_o(\xi a)\left\{\begin{array}{l}\epsilon_r \varphi H_o^{(1)}(\varphi b)[J_o(\xi a)Y_1(\xi b) - J_1(\xi b)Y_o(\xi a)] \\ -\xi H_1^{(1)}(\varphi b)[J_o(\xi a)Y_o(\xi b) - J_o(\xi b)Y_o(\xi a)]\end{array}\right\}}{4[\xi J_o(\xi b)H_1^{(1)}(\varphi b) - \epsilon_r \varphi J_1(\xi b)H_o^{(1)}(\varphi b)]} \tag{13}$$

In order to invert (13) from the k-domain into the real z-domain, the singularities of (13) on the complex k-plane must be carefully investigated. Similar to Section IIB, there are only two branch points at $k = \pm k_o$. Points at $k = \pm k_1$ are not branch points, but are two simple poles. This can be recognized easily by employing small argument expansion for Bessel function with arguments ξa and ξb in (13). The leading term is

$$\lim_{k \to \pm k_1} \bar{G}_2(k, a) = \lim_{k \to \pm k_1} \frac{\mu_o \epsilon_r \varphi H_o^{(1)}(\varphi b)}{\pi b(k_1^2 - k^2)[2H_1^{(1)}(\varphi b) - \epsilon_r \varphi b H_o^{(1)}(\varphi b)]} \tag{14}$$

The numerator of (13) is again the characteristic equation of a Goubau wave given by (17) in the previous section; therefore, (13) has two zeros at $k = \pm k_s$. Other poles can be found by locating the zeros of the denominator. If the branch cuts are drawn in the same manner as

before (Figure 9), and the same steps are followed as discussed in Section IIB, similar conclusion can be drawn.

(a) There is no pole on the real axis in the range $k_1 < |k| < \infty$. In this range the denominator of (13) can be expressed as $-\frac{i}{\pi}[\alpha\epsilon_o I_o(\alpha b)K_1(\beta b) + \beta\epsilon_1 I_1(\alpha b)K_o(\beta b)]$, where K and I are modified Hankel and Bessel functions, α and β are defined by (26) in Section II. The quantity within the bracket is always greater than zero.

(b) There is no pole on the real axis in the range $k_o < |k| < k_1$ for $\sqrt{k_1^2 - k^2}\, b < 2.405$. In this range, the vanishing of the denominator requires that

$$\xi J_o(\xi b)K_1(\beta b) - \epsilon_r \beta J_1(\xi b)K_o(\beta b) = 0 \qquad (15)$$

Equation (15) is the characteristic equation of a dielectric wave guide [11] (p. 263). The lowest cutoff frequency is at $\sqrt{k_1^2 - k^2}\, b = 2.405$. No mode is excited or no pole exists in this portion of the real axis for $\sqrt{k_1^2 - k^2}\, b < 2.405$.

(c) There is no pole on either side of the branch cuts. The arguments are the same as those in Section IIB(c). That is, the real quantity $\frac{\xi J_o(\xi b)}{\epsilon_1 \varphi J_1(\xi b)}$ can not equal the complex quantity $H_o^{(1)}(\varphi b)/H_1^{(1)}(\varphi b)$ on both sides of the branch cuts.

(d) There is no pole in the domain of very large $|k|$ including infinity. For large $|k|$, the denominator behaves like

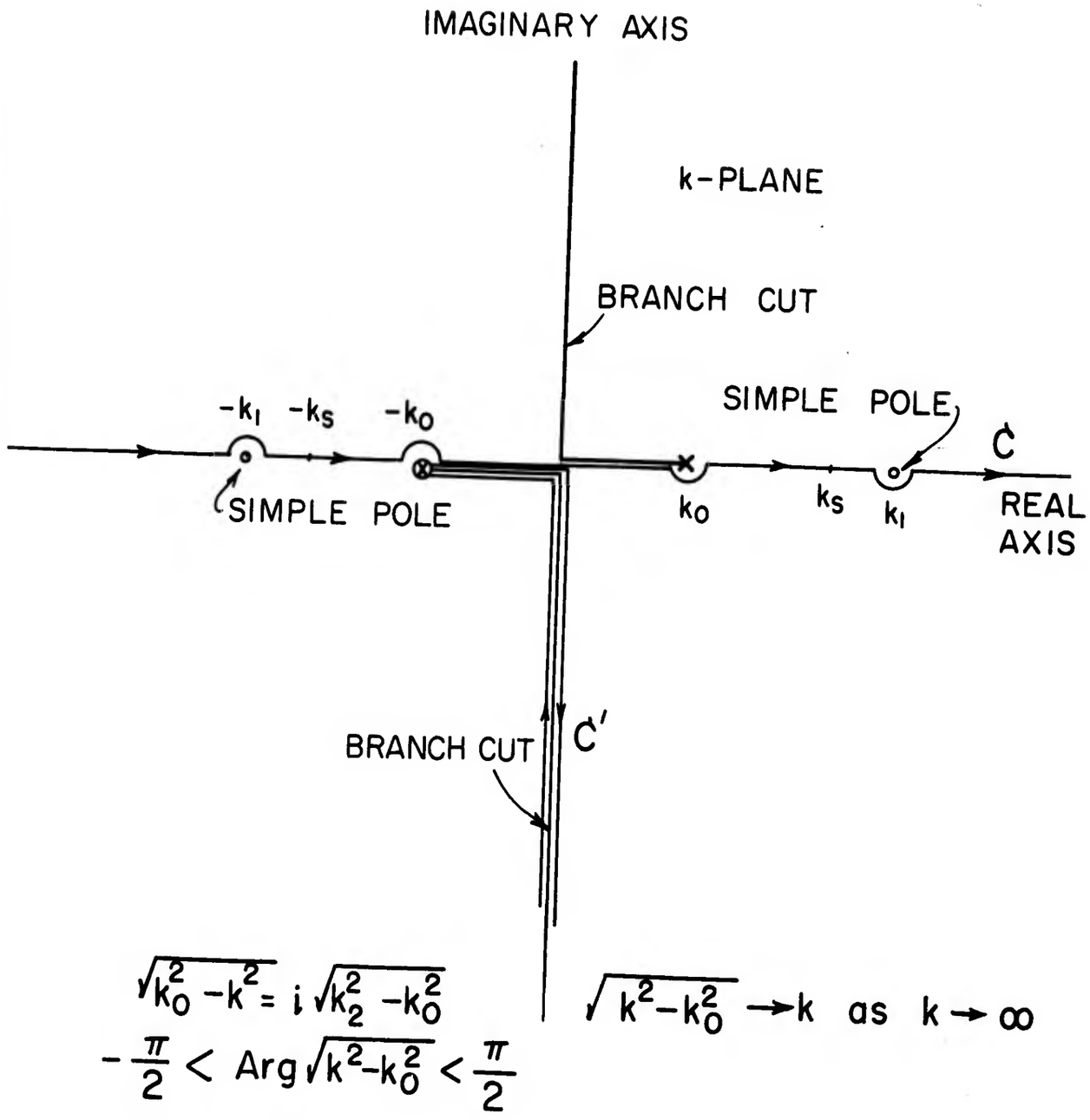

FIG. 9 INTEGRATION PATHS C, C′ AND SINGULARITIES ON k-PLANE

$$\frac{2e^{i(\varphi b-\frac{\pi}{4})}}{\pi b\sqrt{\varphi\xi}}\ \{-i\xi\cos(\xi b-\tfrac{\pi}{4})+\epsilon_r\varphi\sin(\xi b-\tfrac{\pi}{4})\}$$

which has an essential zero right at infinity, but $\overline{G}_2(k,a)$ behaves like

$$\frac{\mu_o\cos(\xi a-\frac{\pi}{4})\{-\epsilon_r\varphi\cos[\xi(b-a)]+i\xi\sin[\xi(b-a)]\}}{2\pi\xi a\{i\xi\cos(\xi b-\frac{\pi}{4})+\epsilon_r\varphi\sin(\xi b-\frac{\pi}{4})\}}$$

which is everywhere finite. Similar to (32-c) in Section II a necessary condition for having a pole is

$$\pm\sqrt{k^2-k_1^2}\,b+i\frac{\pi}{4}=\frac{1}{2}\ell n\frac{1\mp\epsilon_r}{1\pm\epsilon_r}+in\pi \tag{16}$$

which, however, can never be satisfied since the signs of the real parts are different on the two sides.

(e) There is no pole on the finite complex k-plane. The proof is precisely the same as that in Section IIB(e).

With this information and for $z > 0$, by closing the Fourier inverse contour in the lower half plane the Green's function may be expressed as follows:

$$G_2(z,a) = \frac{1}{2\pi}\int_c \bar{G}_2(k,a)\, e^{-ikz}\, dk$$

$$= i\,\frac{\epsilon_r\sqrt{k_1^2 - k_o^2}\, K_o(\sqrt{k_1^2 - k_o^2}\, b)\, e^{ik_1|z|}}{2\pi b k_1 [2K_1(\sqrt{k_1^2 - k_o^2}\, b) + \epsilon_1\sqrt{k_1^2 - k_o^2}\, b\, K_o(\sqrt{k_1^2 - k_o^2}\, b)]}$$

$$+ i\int_o^{k_o} \frac{\mu_o \epsilon_r [J_o(Qa)]^2\, e^{ixz}\, dx}{\pi^3 b^2 \{[QJ_o(Qb)J_1(Pb) - \epsilon_r PJ_1(Qb)J_o(Pb)]^2}$$

$$+ [QJ_o(Qb)Y_1(Pb) - \epsilon_r PJ_1(Qb)Y_o(Pb)]^2\}$$

$$+ \int_o^{\infty} \frac{\mu_o \epsilon_r [J_o(Va)]^2\, e^{-yz}\, dy}{\pi^3 b^2 \{[VJ_o(Vb)J_1(Ub) - \epsilon_r UJ_1(Vb)J_o(Ub)]^2}$$

$$+ [VJ_o(Vb)Y_1(Ub) - \epsilon_r UJ_1(Vb)Y_o(Ub)]^2\} \qquad (17)$$

where

$$Q = \sqrt{k_1^2 - x^2}$$

$$P = \sqrt{k_o^2 - x^2}$$

$$U = \sqrt{k_o^2 + y^2}$$

$$V = \sqrt{k_1^2 + y^2} \qquad (18)$$

The first term comes from the residue at $-k_1$; the second and the third terms come from the branch cut, as shown in Figure 9.

Once the Green's function is known, it is possible to proceed to analyze the finite antenna. As shown in Figure 8(b) a finite tubular dipole is imbedded in an infinite dielectric rod with a delta generator at $z = 0$. From the condition that the tangential electric field vanish on the surface of the antenna, Hallén's integral equation is obtained. It is

$$\frac{4\pi}{\mu_o} A_z = \int_{-h}^{h} I(z')\mathcal{K}(z - z')\, dz' = \frac{i4\pi}{\zeta_1}\left[C\cos k_1 z + \frac{V}{2}\sin k_1 |z|\right] \qquad (19)$$

where

$$\mathcal{K}(z - z') = \frac{2}{\mu_o}\int_{-\infty}^{\infty} \overline{G}_2(k, a)\, e^{-ik(z - z')}\, dk = \frac{4\pi}{\mu_o} G_2(z - z', a) \qquad (20)$$

$$\zeta_1 = \sqrt{\frac{\mu_o}{\epsilon_1}} \qquad (21)$$

and C is a constant to be determined by the condition that the current vanish at $z = \pm h$.

Up to this point, there has been an ambiguity in the inverse Fourier integration in the complex k-plane. The question is, should the contour of integration c, where it meets the poles at $\pm k_1$, go as shown in Figure 9 or in the opposite direction, that is, downward at $-k_1$

and upward at $+k_1$. Although the contribution from this pole contributes nothing to the actual fields, it is important to determine how this difference influences the results obtained from the integral equation (19). This ambiguity can be clarified by the following facts. The contribution to the Green's function $\mathcal{K}(z - z')$ by the pole at $-k_1$ can be expressed as $F(k_1)e^{ik_1|z - z'|}$ where $F(k_1)$ is an odd function of k_1 and is explicitly given by (17). Owing to the symmetry of the current, $I(z) = I(-z)$, it can be proved that

$$\int_{-h}^{h} I(z')\, F(k_1)\, e^{ik_1|z - z'|}\, dz'$$

$$= 2F(k_1) \cos k_1 z \int_{o}^{h} I(z')e^{ik_1 z'}\, dz'$$

$$+ F(k_1)\left[e^{ik_1 z} \int_{o}^{z} I(z')e^{-ik_1 z'}\, dz' - e^{-ik_1 z} \int_{o}^{z} e^{+ik_1 z'}\, dz'\right] \tag{22}$$

The first part on the right-hand side of (22) has nothing to do with current distribution $I(z)$. It only changes the constant c in (19). The second part on the right-hand side of (22) is an even function of k_1, which is independent of the sign of k_1, Consequently, the path of integration c can go either way. The residue at $-k_1$ or k_1 gives the same answer for the current distribution.

B. A Numerical Method

Equation (19) is an exact integral equation for the model shown in Figure 9. When $k_1 b \ll 1$ the small-argument expansion of the Bessel functions can be used to approximate the kernel. This is discussed by Wu [1]. The kernel has been expressed in a form similar to that of the kernel of a dipole in free space but with a slightly modified radius and a surface impedance. Accordingly, the prediction can be made that the current distribution when both the antenna and the coating are very thin should be close to that of a free-space dipole. On the other hand, it is more interesting to know the change in the current distribution when the coating gets thicker. This is the main purpose of the investigation in this section. Since no simple approximation can be made for the kernel, it is difficult to obtain even an approximate solution. The method employed here is a numerical one given by Andrew Young [12], [13]. In his two papers, first integrals of the product of two functions $f(x)$ and $\phi(x)$ are expressed in the form

$$\int_a^b f(x)\, g(x)\, dx = \sum_{r=1}^{n} \gamma_r f(x_r) + R \qquad (23)$$

where $x_1, x_2, \ldots x_n$ are the n abscissae with which are associated weights $\gamma_1, \gamma_2, \ldots \gamma_n$; R is a correction term. It has been shown that by expanding $f(x)$ in a Taylor's series about the mid-point of the

interval between a and b, and by equally spacing the n abscissae that is $x_n - x_{n-1} = x_{n-1} - x_{n-2} = \cdots = x_2 - x_1 = t$, the γ's can be expressed in a matrix form. For instance, for n = 3, they are

$$\begin{bmatrix} \gamma_1 \\ \gamma_2 \\ \gamma_3 \end{bmatrix} = \frac{1}{2} \begin{bmatrix} 0 & -1 & 1 \\ 2 & 0 & -2 \\ 0 & 1 & 1 \end{bmatrix} \begin{bmatrix} \mu_1 \\ \mu_2 \\ \mu_3 \end{bmatrix} \tag{24}$$

where

$$\mu_s = \frac{1}{t^s} \int_a^b (x - x_2)^s g(x)\, dx \tag{25}$$

$$s = 0,\ 1,\ 2$$

The remainder term R is proportional to the fourth derivative of f(x) within the interval. The next step is to apply the approximate product-integration (23) to the numerical solution of integral equations. To begin with, because of the symmetry of the current $I(z) = I(-z)$, (10) may be rewritten as

$$\int_o^h I(z') \left[\mathcal{K}(z - z') + \mathcal{K}(z + z') \right] dz' = \frac{i4\pi}{\zeta_1} \left[C \cos k_1 z + \frac{V}{2} \sin k_1 |z| \right] \tag{26}$$

The interval (0, h) may be divided into ℓ sub-intervals. Within each sub-interval, an approximation of the type (23) is used. That is, by expanding the current $I(z)$ in each sub-interval into a quadratic form (or $n = 3$) about the mid-point of the sub-interval, the right-hand side of (26) becomes:

$$\int_0^h I(z')\left[\mathcal{K}(z-z') + \mathcal{K}(z+z')\right] dz'$$

$$= \left\{\int_0^{2t} + \int_{2t}^{4t} + \int_{4t}^{6t} + \cdots + \int_{2(\ell-1)t}^{2\ell t}\right\} I(z')\left[\mathcal{K}(z-z') + \mathcal{K}(z+z')\right] dz'$$

$$= \sum_{j=1}^{\ell} \left\{\gamma_1^j(z)\, I[(2j-2)t] + \gamma_2^j(z)\, I[(2j-1)t] + \gamma_3^j(z)\, I[2jt]\right\} \tag{27}$$

where $t = \frac{h}{2\ell}$

By defining

$$\mu_n(mt) = \frac{1}{t^{n-1}} \int_{-t}^{t} z'^{n-1}\, \mathcal{K}(mt - z')\, dz'$$

$$= (-1)^{n-1}\, \mu_n(-mt) \tag{28}$$

$$n = 1,\ 2,\ 3;\ m = 0,\ 1,\ \ldots\ 4\ell-1$$

all the γ's in (27) can be expressed in terms of the μ's. According to the relation (24), they are

$$\gamma_1^j(z) = \frac{1}{2}\{-\mu_2[z-(2j-1)t] + \mu_2[z+(2j-1)t] + \mu_3[z-(2j-1)t] + \mu_3[z+(2j-1)t]$$

$$\gamma_2^j(z) = \mu_1[z-(2j-1)t] + \mu_1[z+(2j-1)t] - \mu_3[z-(2j-1)t] + \mu_3[z+(2j-1)t]$$

$$\gamma_3^j(z) = \frac{1}{2}\{\mu_2[z-(2j-1)t] - \mu_2[z+(2j-1)t] + \mu_3[z-(2j-1)t] + \mu_3[z+(2j-1)t]\} \quad (29)$$

Now let $z = mt$ in (26) together with (27) and let m change from 0 to 2ℓ. In this manner a set of $2\ell+1$ linear equations are generated with $2\ell+1$ unknowns. Since the current vanishes at $z = 2\ell t$, there are only 2ℓ unknowns for the current plus an unknown constant C. In matrix notation

$$[A][I] = [G] \quad (30)$$

where [I] and [G] are $2\ell+1$ by 1 column matrices

$$[I] = \begin{bmatrix} I(0) \\ I(t) \\ I(2t) \\ \vdots \\ I(2\ell t - t) \\ C \end{bmatrix} \qquad [G] = \frac{i2\pi V}{\zeta_1} \begin{bmatrix} 0 \\ \sin(k_1 t) \\ \sin(2k_1 t) \\ \vdots \\ \sin(2\ell k_1 t) \end{bmatrix} \tag{31}$$

and $[A]$ is a $2\ell+1$ by $2\ell+1$ square matrix whose elements $A_{p,q}$ are given by

$$q = 1 \qquad A_{p,1} = \gamma_1^1(pt) \tag{32-a}$$

$$q = \text{even number} \qquad A_{p,q} = \gamma_3^{q/2}(pt) + \gamma_1^{q/2+1}(pt) \tag{32-b}$$

$$q = \text{odd number} \qquad A_{p,q} = \gamma_2^{(q+1)/2}(pt) \tag{32-c}$$

$$q = 2\ell+1 \qquad A_{p,2\ell+1} = \frac{i4\pi}{\zeta_1} \cos(pk_1 t) \tag{32-d}$$

The γ's are given by (28); they are all complex quantities. If the square matrix $[A]$ is inverted, the numerical value of the current and constant C are immediately obtained. Thus:

$$[I] = [A]^{-1}[G] \tag{33}$$

It is noted, that all of the constants μ given by (28) are in double integral form. By interchanging the order of integration, one of them

can be carried out easily and the other is left for the computer. Explicit formulas for the μ's are given in Appendix 3.

C. Numerical Results

Computations have been done by an I. B. M. Computer 7094. Since many integrations of Bessel functions are involved in generating the constants μ and then the matrix elements $A_{p,q}$, a considerable length of time is required in order to achieve one curve of the current distribution. Fortunately, a way has been found which can save much computing time and give a number of curves simultaneously. Beginning with the longest antenna to be investigated, the length h is divided into ℓ subdivisions as described before, and the $2\ell+1$ by $2\ell+1$ matrix [A] is formed. Then, for shorter antennas with length $h - (\frac{h}{\ell})n$, $n = 1, 2, \ldots \ell-1$, the matrix elements $A_{p,q}$ in each case are precisely the same as before except in the last column, which should always keep cosine terms. The only significant change is that the order of the matrix shrinks by two each time n is increased by 1. Consequently, once the $2\ell+1$ by $2\ell+1$ matrix is formed, by redefining the last column each time, the current distributions for ℓ different lengths are obtained almost simultaneously.

Some typical results have been obtained for $\epsilon_r = 3.00$, $k_o a = 0.04$, $k_o h = 0.75$, $\ell = 24$, and three different thicknesses of the dielectric coating, namely, $b/a = 2$, 4, and 8. For each set of

values a 49 x 49 [A] matrix was formed and then enverted step by step. The current distributions for 24 different lengths have been obtained, of which only $k_o h = \frac{\pi}{4}, \frac{\pi}{2}, \frac{3}{4}\pi$ are shown in Figures 10 to 12. Also shown in Figures 10 and 11 are the experimental curves by David Lamensdorf*. They provide an excellent check on the theory. Note that when the antenna becomes longer, beautiful standing waves are formed along them as shown in Figure 12. The wavelengths are close to the surface-wave length especially when b/a is large. This agrees with the results of Section I, that the current in a dielectric-coated infinite cylindrical antenna is primarily the transmission current and not the radiation current when the coating is reasonably thick.

Another interesting part of the results is the input admittance. Since calculations are based upon the assumption that the voltage across the delta generator is 1, the real part of the current at $z = 0$ is the input conductance, and the imaginary part at $z = 0$ is the input susceptance. Figure 13 shows the curves of the input admittances as the length of the antenna changes. Experimental points by David Lamensdorf are superimposed on them. It is noted, that the input conductances agree very well, but not the input susceptances. The reason is simple. Since a delta generator at $z = 0$ was assumed, the input susceptances should theoretically be infinite at $z = 0$ as discussed

* The experimental data are obtained from David Lamensdorf who used a dielectric sleeve which was much longer than the antenna itself and in close contact with it. Experimental results show that the length of the sleeve is not important, so long as it is much longer than the antenna. [16]

in Section IIC. Therefore, the more points are taken in the calculation of the current distribution, the higher the input susceptance will be. Nevertheless, the general shape of the input susceptance curve, obtained in the manner previously described, is still good. If one point is calibrated the rest are known.

Comparisons with free-space dipoles [14] are also interesting. In general, the input conductances are larger for dielectric-coated antennas, and the input susceptances are more inductive. This is because the antenna is effectively thicker in the dielectric rod than in free space. The resonant and anti-resonant lengths are shorter for dielectric-coated antennas. In other words, the effective length of an antenna in a dielectric rod is greater than that in free space as was anticipated before doing any calculations.

There is an interesting characteristic for the case $b/a = 8$. The second resonant peak is greater than the first resonant peak, as shown in Figure 13, which also agrees with experiment. The explanation is that when $b/a = 8$ the transmission current is a much more important part of the total current than when b/a is nearer 1. After a sequence of reflections at each end, a standing wave is produced along the antenna. The resonant peak occurs when a maximum is located at $z = 0$, if the radiation current is completely neglected. Actually, this is not the whole story, because whenever the transmission current is reflected at an end it gives rise to a radiation

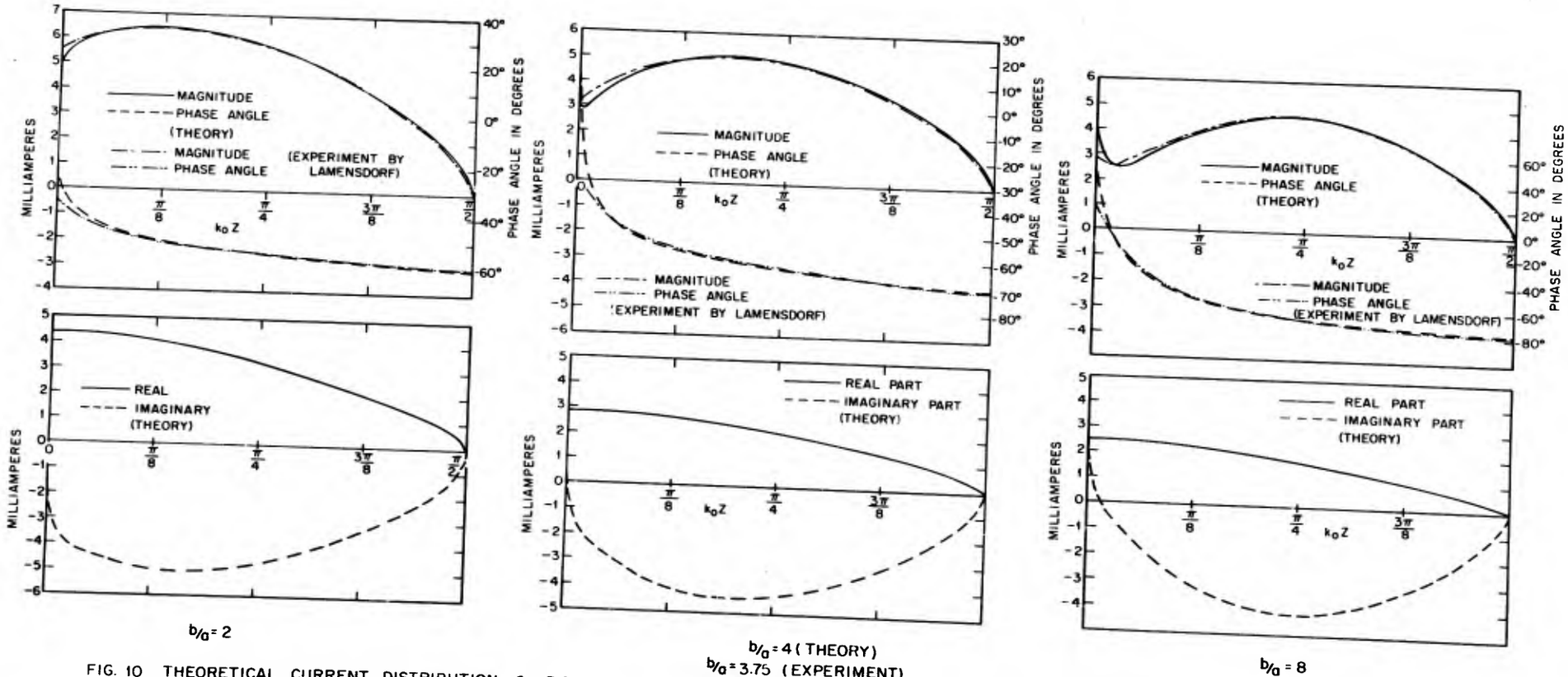

b/a = 2

b/a = 4 (THEORY)
b/a = 3.75 (EXPERIMENT)

b/a = 8

FIG. 10 THEORETICAL CURRENT DISTRIBUTION $\epsilon_r = 3.0$, $k_0 a = 0.04$, $k_0 h = \pi/2$ AND EXPERIMENTAL CURRENT DISTRIBUTION $\epsilon_r = 3.2 < .02$, $k_0 a = 0.04$, $k_0 h = \frac{\pi}{2}$

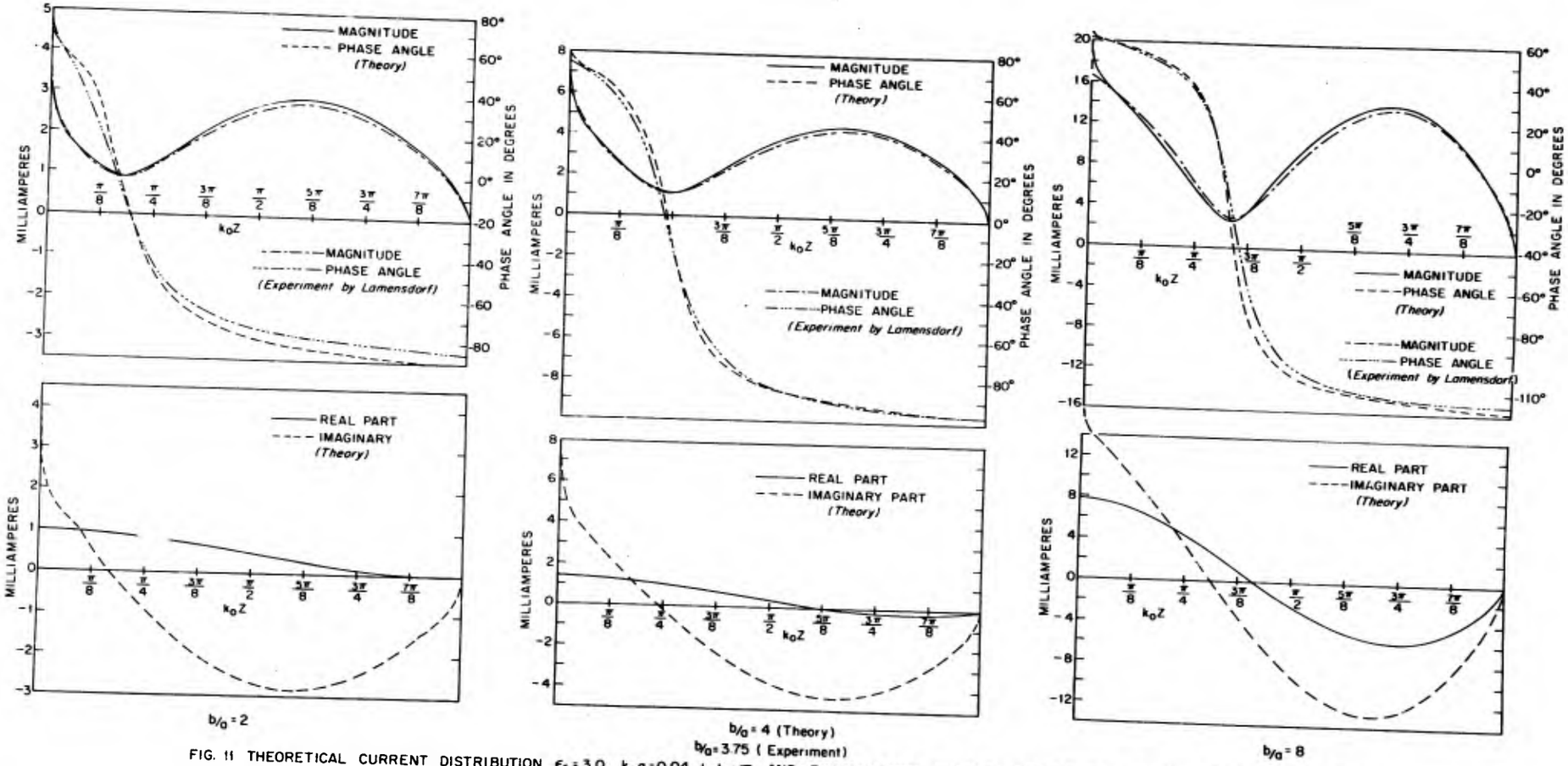

FIG. 11 THEORETICAL CURRENT DISTRIBUTION $\epsilon_r = 3.0$, $k_0 a = 0.04$, $k_0 h = \pi$, AND EXPERIMENTAL CURRENT DISTRIBUTION $\epsilon_r = 3.2 \angle .02$, $k_0 a = 0.04$, $k_0 h = \pi$.

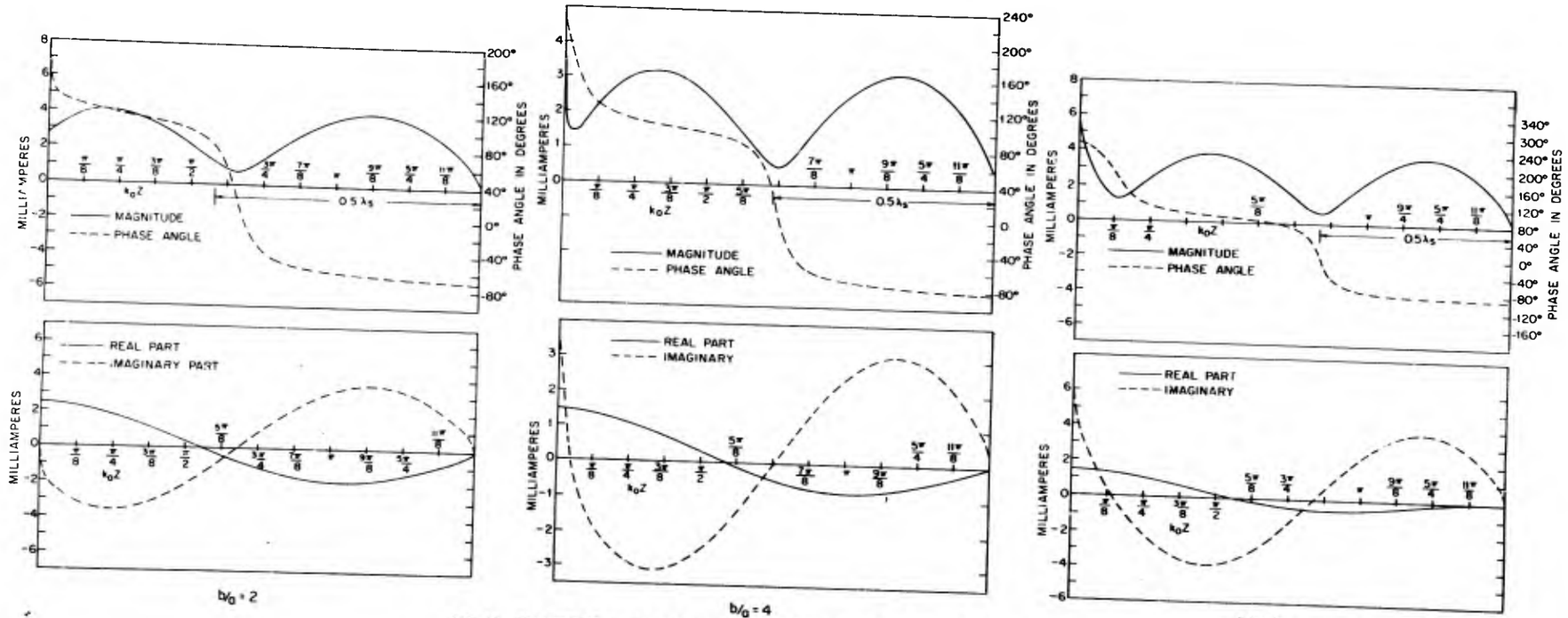

FIG 12 THEORETICAL CURRENT DISTRIBUTION $\epsilon_r = 3.0$, $k_0 a = 0.04$, $k_0 h = 3/2\,\pi$

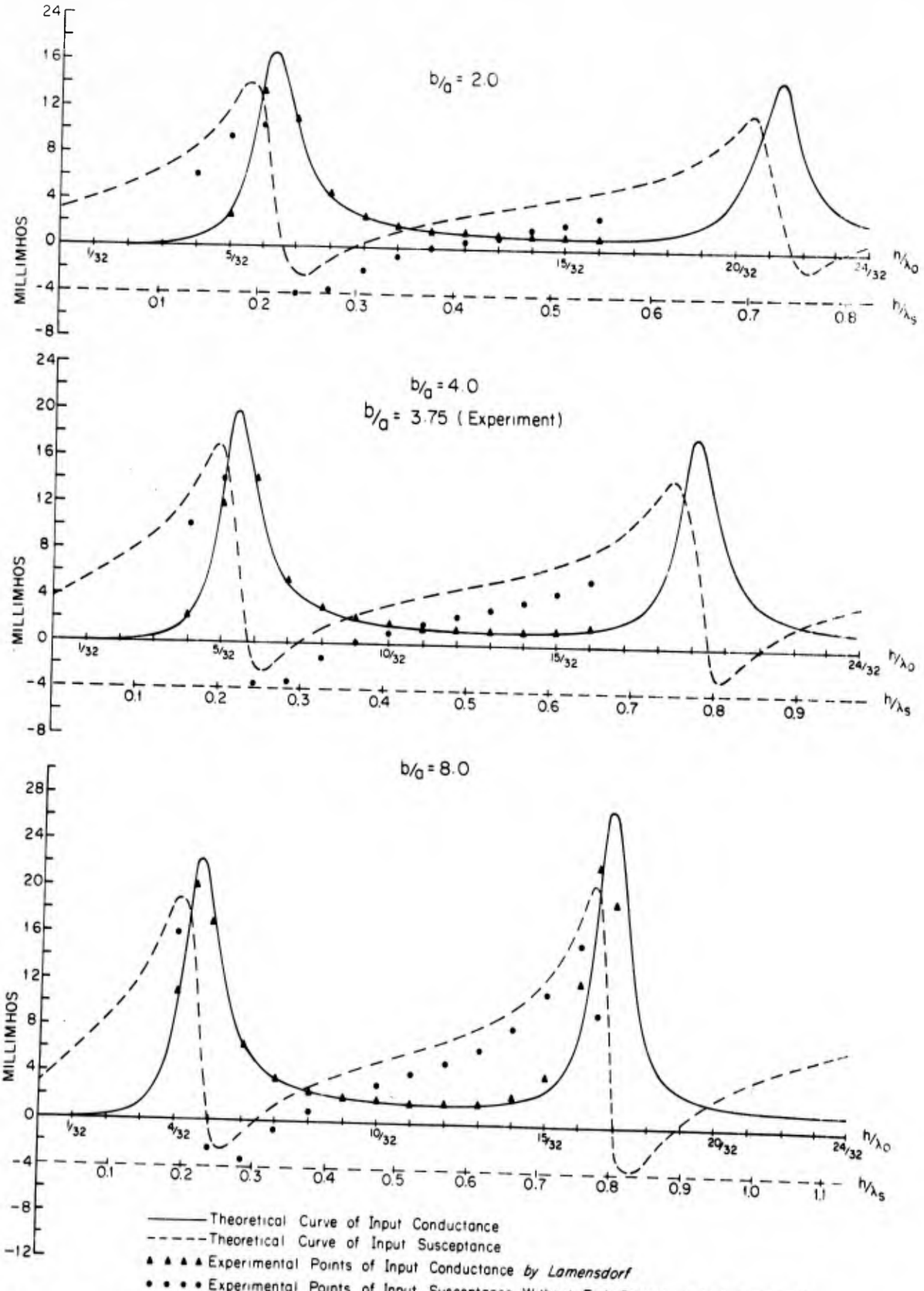

FIG. 13 THEORETICAL INPUT ADMITTANCE $\epsilon_r = 3.0$, $k_0a = 0.04$ AND EXPERIMENTAL INPUT ADMITTANCE $\epsilon_r = 3.2 < .02$, $k_0a = 0.04$

current. Therefore, two kinds of standing waves exist along the line. At the second resonance, the antenna is quite long; the radiation current originating at the ends dies out quickly, so the standing wave of the radiation current is very small at $z = 0$. It has little influence on the peak of the transmission current at $z = 0$. However, for the first resonance, the antenna is quite short and the standing wave of the radiation current is not small at $z = 0$. It partially cancels the standing wave of the transmission current near $z = 0$; a reduced maximum is the result.

D. Second Solution—Approximating the Current by Two Terms

A study of the curves of the current distribution obtained by the numerical method shows that their general shapes are similar to those of the current in dipoles in free space. The real part is mainly a shifted cosine term, and the imaginary part is mainly a sine term, though the wavelength is no longer the free-space wavelength, but seems to be more nearly the surface-wavelength. Attempts were made to find an approximate current which contains these two terms only.

The use of two terms to approximate the current distribution of a free-space dipole, first discussed by King [15], was based upon the principle that the real part of the kernel of the integral equation behaves like a delta function, so the current should behave more or

less like the right-hand side of the integral equation. Checking the kernel in integral equation (19), $K(z - z')$ given by (20) does not have this property. Because of the residue from the simple pole at $k = -k_s$, $K(z - z')$ has a term with constant amplitude independent of z. In order to make the method applicable, some kind of modification is needed. In fact, the integral equation of a finite dielectric-coated antenna given by (19) is not a unique form. More generally, (10) can be written as

$$\int_{-h}^{h} I(z')\, K'(z - z')\, dz' = \frac{i4\pi}{\zeta_2}\left[C\cos k_2 z + \frac{V}{2}\sin k_2 z\right] \tag{34}$$

where k_2 can be any arbitrary propagation constant and

$$\zeta_2 = \zeta_o \frac{k_o}{k_2} \tag{35}$$

$K'(z - z')$, differs slightly from $K(z - z')$; it is given by

$$K'(z - z') = \frac{2}{\mu_o}\int_{-\infty}^{\infty} \frac{k_2^2(k^2 - k_1^2)}{k_1^2(k^2 - k_2^2)}\, \overline{G}_2(k, a)\, e^{-ik|z - z'|}\, dk \tag{36}$$

Equation (34) can be verified easily either by taking a Fourier transform on both sides or by adding a second layer with dielectric constant ϵ_2 and propagation constant k_2 just outside the conducting cylinder and taking the limit as the thickness of this artificial layer goes to zero.

The singularities of $\overline{G}_2(k, a)$ have been studied in Part A of this section. They consist of two branch points at $k = \pm k_o$, two simple poles at $k = \pm k_1$, and two zeros at $k = \pm k_s$. Accordingly, if one choses $k_2 = k_s$ in (36), then the integrand has neither a pole nor a zero in the complex k-plane. The only singularities left will be two branch points and two branch cuts associated with them, which are very similar to the free space Green's function. The Green's function $h\mathcal{K}'(z - z')$ is shown in Figure 14 with $k_2 = k_s$ for $\epsilon_r = 3.00$, $k_o a = 0.04$, and three different values of b/a, namely, 2, 4, and 8.

As for the free-space dipole, an equivalent form of (34) is [15]

$$\int_{-h}^{h} I(z')\mathcal{K}_d(z - z') = \frac{i4\pi}{\zeta_s \cos k_s h}\left[UF_{0z} + \frac{1}{2} VM_{oz}\right] \tag{37}$$

where

$$\mathcal{K}_d(z, z') = \mathcal{K}'(z - z') - \mathcal{K}'(h - z') \tag{38}$$

$$U = \frac{i\zeta_s}{4\pi}\int_{-h}^{h} I(z')\mathcal{K}'(h - z')\, dz' \tag{39}$$

$$M_{oz} = \sin(k_s h - k_s |z|) \tag{40}$$

$$F_{oz} = \cos k_s z - \cos k_s h \tag{41}$$

$$\zeta_s = \zeta_o \frac{k_o}{k_s} \tag{42}$$

Let it be assumed that an approximate current has the form

$$I(z) = \frac{2\pi}{\zeta_s \cos k_s h} \left[T_a M_{oz} + T_b F_{oz} \right] \tag{43}$$

where T_a and T_b are two complex constants to be determined. Let

$$\int_{-h}^{h} dz' F_{oz'} \mathcal{K}_d(z, z') = \Psi_{duu} F_{oz} + \Psi_{duv} M_{oz} + \gamma_1(z) \tag{44}$$

$$\int_{-h}^{h} dz' M_{oz'} \mathcal{K}_d(z, z') = \Psi_{dvu} F_{oz} + \Psi_{dvv} M_{oz} + \gamma_2(z) \tag{45}$$

where $\gamma_1(z)$, $\gamma_2(z)$ are small. If $\gamma_1(z)$ and $\gamma_2(z)$ are neglected and (32) and (33) are matched at $z = 0$ and $z = h - \frac{\pi}{2k_s}$, all of the Ψ constants can be determined. Also define

$$\Psi_v = \int_{-h}^{h} M_{oz} \mathcal{K}'(h, z') \, dz' \tag{46}$$

$$\Psi_u = \int_{-h}^{h} F_{oz} \mathcal{K}'(h, z') \, dz' \tag{47}$$

If the approximate current (43) is substituted in (37) and (39) and use is made of the relations (44), (45), (46), and (47), the constants T_a and T_b can be evaluated. They are:

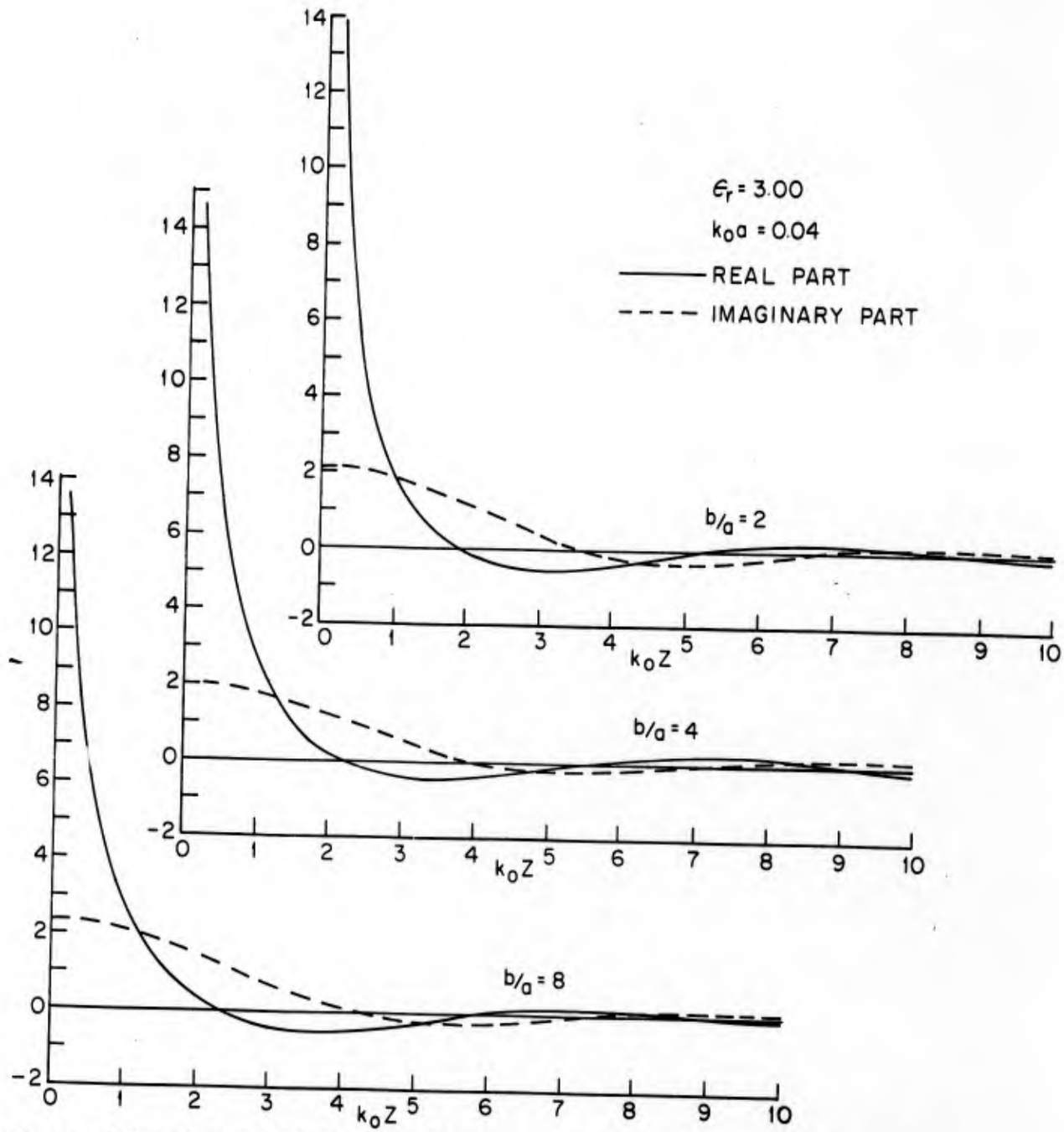

FIG. 14 GREEN'S FUNCTIONS, $h\mathcal{K}'(z)$, WITH $\epsilon_r = 3.0$, $k_0 a = 0.04$, $k_0 h = 3/4\,\pi$

$$T_a = \frac{i\left(\Psi_{duu} - \frac{\Psi_u}{\cos k_s h}\right)}{\left(\Psi_{dvu} - \frac{\Psi_v}{\cos k_s h}\right)\Psi_{duv} - \left(\Psi_{duu} - \frac{\Psi_u}{\cos k_s h}\right)\Psi_{dvv}} \tag{48}$$

$$T_b = \frac{-i\left(\Psi_{dvu} - \frac{\Psi_v}{\cos k_s h}\right)}{\left(\Psi_{dvu} - \frac{\Psi_v}{\cos k_s h}\right)\Psi_{duv} - \left(\Psi_{duu} - \frac{\Psi}{\cos k_s h}\right)\Psi_{dvv}} \tag{49}$$

Calculations have been made for three cases:

(a) $\epsilon_r = 3.00$, $k_o a = 0.03990$, $k_o h = 0.375\pi$, $b/a = 2$. It is found that $k_s/k_o = 1.0959$, $k_s h = 2.582$.

$$I(z) = -0.0216[(-0.0024 - i\,0.155)M_{oz} + (0.0287 - i\,0.0307)F_{oz}] \tag{50}$$

(b) $\epsilon_r = 3.00$, $k_o a = 0.03990$, $k_o h = 0.375\pi$, $b/a = 4$. It is found that $k_s/k_o = 1.3010$, $k_s h = 3.066$.

$$I(z) = -0.0217[(-0.0011 - i\,0.175)M_{oz} + (0.0216 - i\,0.0399)F_{oz}] \tag{51}$$

(c) $\epsilon_r = 3.00$, $k_o a = 0.3990$, $k_o h = 0.375\pi$, $b/a = 8$. It is found that $k_s/k_o = 1.5128$, $k_s h = 3.563$.

$$I(z) = -0.0276[(+0.0025 - i\,0.200)M_{oz} + (0.0313 - i\,0.0387)F_{oz}] \tag{52}$$

Graphs for the cases (a), (b), and (c) are shown in Figure 15. At the same time, comparisons are made with curves obtained by the numerical method. The agreement is only fairly good because the Green's function shown in Figure 14 is not as ideal as that in free space. The real part of the Green's function in free space approximates a delta function more closely. It rises steeply toward the source point and falls off rapidly to zero at $k_o z = 1.5$, whereas in the present case, the rise toward the source point is less steep and decreases to zero at $k_o z = 2$ or greater as b/a increases. In terms of $k_s z$ it is even larger. This also explains why the case $b/a = 8$ is less satisfactory than others. However, the results are good enough to calculate the far field or field patterns in the engineering sense. These are discussed in the next part. Explicit formulas for the Ψ's are listed in Appendix 4.

E. Field Patterns

Once the current is known, the far field and field pattern can be calculated easily. The transformed vector potential in region III $\overline{G}_3(k, r)$ due to a ring delta source is given by (12), so that the θ-component of the magnetic field in this region due to this ring delta source can be expressed as follows:

$$-\frac{\partial \overline{G}_3(k, r)}{\partial r} = \frac{\xi \mu_o J_o(\xi a) H_1^{(1)}(\varphi r)}{2\pi b[\xi J_o(\xi b) H_1^{(1)}(\varphi b) - \epsilon_r \varphi J_1(\xi b) H_o^{(1)}(\varphi b)]} \qquad (53)$$

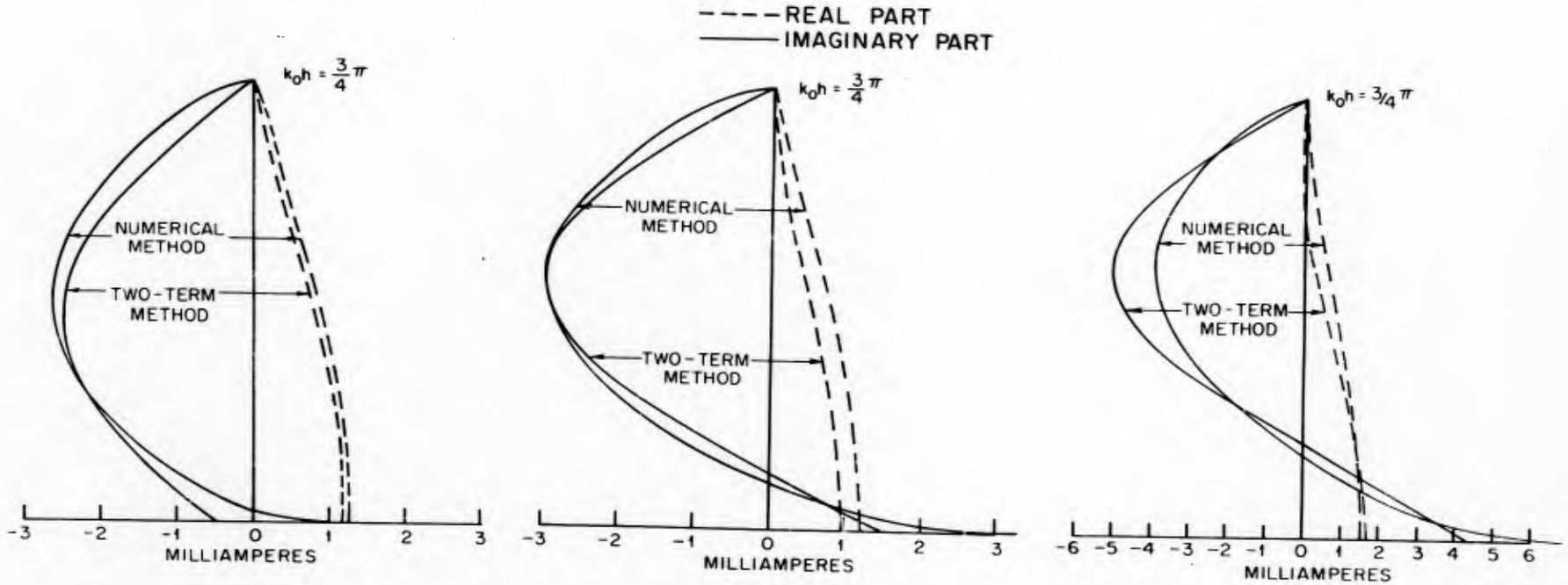

$b/a = 2$
$k_s h = 2.58$

$b/a = 4$
$k_s h = 3.06$

$b/a = 8$
$k_s h = 3.56$

FIG. 15 A COMPARISON OF CURRENT DISTRIBUTION BY TWO-TERM METHOD TO NUMERICAL METHOD $\epsilon_r = 3.0$, $k_0a = 0.04$, $k_0h = 3/4\,\pi$.

The actual magnetic field due to this ring delta source is the inverse Fourier transform of (53). By superposition, the total magnetic field $B_{3\theta}$ due to current in the whole antenna is

$$B_{3\theta} = \int_{-h}^{h} I(z')\,dz' \int_{C} \frac{dk \;\; \xi\mu_o J_o(\xi a) H_1^{(1)}(\varphi r)\, e^{-ik(z-z')}}{4\pi^2 b[\xi J_o(\xi b) H_1^{(1)}(\varphi b) - \epsilon_r \varphi J_1(\xi b) H_o^{(1)}(\varphi b)]} \tag{54}$$

It is now convenient to change to spherical coordinates (R, $\textcircled{H}$, ϕ), with $Z = R\cos\textcircled{H}$, $r = R\sin\textcircled{H}$ in (54). Then, as $R\to\infty$ (54) becomes

$$\lim_{R\to\infty} B_{3\theta} = \lim_{R\to\infty} \int_{-h}^{h} I(z')\,dz' \int_{C} \frac{\xi\mu_o J_o(\xi a) e^{ikz'} e^{-i\frac{3}{4}\pi}}{4\pi^2 b[\xi J_o(\xi b) H_1^{(1)}(\varphi b) - \epsilon_r \varphi J_1(\xi b) H_o^{(1)}(\varphi b)]}$$

$$\times \sqrt{\frac{2}{\pi\varphi R\sin\textcircled{H}}}\; e^{iR(\varphi\sin\textcircled{H} - k\cos\textcircled{H})}\, dk \tag{55}$$

The method of steepest descents already used in Section IID applies. The evaluation of the integral (55) at the saddle point $k = -k_o\cos\textcircled{H}$, gives

$$\lim_{k\to\infty} B_{3\theta} = \frac{e^{ik_oR}}{2\pi R} \left[\frac{-\xi\mu_o J_o(\xi a)}{\pi[\xi b J_o(\xi b) H_1^{(1)}(\varphi b) - \epsilon_r \varphi b J_1(\xi b) H_o(\varphi b)]}\right]_{k=-k_o\cos\textcircled{H}}$$

$$\times \int_{-h}^{h} I(z') e^{-ik_oz'\cos\textcircled{H}}\, dz' \tag{56}$$

The Poynting vector in the far field and the radiation factor are defined by (50) and (51) in Section II. If the field factor is defined as the square root of the radiation factor, it can be expressed as follows:

$$F_r(\textcircled{H}) = \frac{4\sqrt{15}\pi R}{\mu_o} |B_{3\theta}| \tag{57}$$

Three different methods are considered in obtaining the field pattern by (57).

(a) Use can be made of the numerical solution obtained in Part C. This again involves the approximate method described in Part B of dividing the antenna into ℓ subdivisions (same number as before). Within each subdivision the current is approximated by a quadratic form, and the integral involved in (56) can be put in the form (23) with $n = 3$. The final result is

$$F_r(\textcircled{H}) = \left| \frac{2\sqrt{15}\,\xi t J_o(\xi a)}{\pi[\xi b J_o(\xi b) H_1^{(1)}(\varphi b) - \epsilon_r \varphi b J_1(\xi b) H_o^{(1)}(\varphi b)]} \right|_{k=-k_o\cos\theta}$$

$$\times \left| \sum_{j=1}^{\ell} [\gamma_1^j I(2jt-2t) + \gamma_2^j I(2jt-t) + \gamma_3^j I(2jt)] \right| \tag{58}$$

where $t = \frac{h}{2\ell}$ as before and

$$\gamma_1^j = -\mu_2(j) + \mu_3(j) \tag{59-a}$$

$$\gamma_2^j = 2\mu_1(j) - 2\mu_3(j) \tag{59-b}$$

$$\gamma_3^j = \mu_2(j) + \mu_3(j) \tag{59-c}$$

$$\mu_1(j) = \frac{1}{\omega}\{\sin(2j\omega) - \sin[(2j-2)\omega]\} \tag{60-a}$$

$$\mu_2(j) = \frac{1}{\omega^2}\{\cos(2j\omega) + \omega\sin(2j\omega) - \cos[(2j-2)\omega] + \omega\sin[(2j-2)\omega]\} \tag{60-b}$$

$$\mu_3(j) = \frac{1}{\omega^3}\{2\omega\cos(2j\omega) + (\omega^2-2)\sin(2j\omega) + 2\omega\cos[(2j-2)\omega] - (\omega^2-2)\sin[(2j-2)\omega]\} \tag{60-c}$$

$$\omega = tk_o\cos\textcircled{H} \tag{61}$$

The currents I(mt), m = 0, 1, . . . 2ℓ, are replaced by the numerical values obtained from Part C.

(b) The two-term solution obtained in Part D may be introduced. If the current in (56) is replaced by the approximate current in (43), the result obtained from (57) is

$$F_r(\textcircled{H}) = \left| \frac{4\sqrt{15}\ \xi h J_o(\xi a)}{\zeta_s \cos(k_s h)[\xi b J_o(\xi b) H_1(\varphi b) - \epsilon_r \varphi b J_1(\xi b) H_o^{(1)}(\varphi b)]} \right|_{k = -k_o \cos\textcircled{H}}$$

$$\times \quad |T_a F_m(\textcircled{H}) + T_b G_m(\textcircled{H})| \qquad (62)$$

where

$$F_m(\textcircled{H}) = \frac{1}{h} \int_{-h}^{h} M_{oz'} e^{-ik_o z' \cos\textcircled{H}}\, dz'$$

$$= \frac{2k_s h[\cos(k_o h \cos\textcircled{H} - \cos k_s h]}{k_s^2 h^2 - k_o^2 h^2 \cos^2\textcircled{H}} \qquad (63)$$

$$G_m(\textcircled{H}) = \frac{1}{h} \int_{-h}^{h} F_{oz'} e^{-ik_o z' \cos\textcircled{H}}\, dz'$$

$$= \frac{2k_s h[k_o h \sin(k_s h) \cos(k_o h \cos\textcircled{H}) \cos\textcircled{H} - k_s h \cos(k_s h) \sin(k_o h \cos\textcircled{H})]}{(k_s^2 h^2 - k_o^2 h^2 \cos^2\textcircled{H}) k_o h \cos\textcircled{H}}$$

(64)

(c) The two-term solution obtained in Part D, may be used without including the contribution from the polarization in the dielectric rod (or the n·p term on its surface). This can be accomplished simply if the free-space Green's function is used to calculate the field, which is

$$B_{3\theta}(R\to\infty) \sim \frac{-i\mu_o k_o \sin\textcircled{H} e^{ik_o R}}{4\pi R} \int_{-h}^{h} I(z') e^{-ik_o z' \cos\textcircled{H}}\, dz' \tag{65}$$

If $I(z')$ is replaced by the approximate current in (43), the field factor (57) becomes

$$F_r(\textcircled{H}) = \frac{2\sqrt{15}\,\pi k_o h \sin\textcircled{H}}{\zeta_s \cos k_s h} \left| T_a F_m(\textcircled{H}) + T_b G_m(\textcircled{H}) \right| \tag{66}$$

where $F_m(\textcircled{H})$ and $G_m(\textcircled{H})$ are the same functions defined in (63) and (64) respectively.

Numerical calculations have been carried out with each of the above three methods for three antennas with dielectric layers of different thicknesses. Their two-term approximate currents are listed in Part D. The results are shown in Figure 16. The study of these curves and of the differences among (a), (b), and (c) shows that the field patterns obtained by the three different methods have the same shapes; but that their magnitudes differ somewhat. The field pattern for the dielectric-coated antenna has greater broadside characteristics than the free-space dipole, and this property becomes more prominent as the dielectric is made thicker. Although a part of the imaginary part of the current has a reversed sign, there is no minor lobe because the antenna is still shorter than one wavelength in free space. The contribution to the field by the time-varying polarization in the dielectric

rod is very small compared with that by the current in the antenna itself (the difference between (b) and (c)), and this difference is roughly proportional to the thickness of the dielectric layer. If the dielectric layer is not extremely thick, as in cases previously discussed, the contribution by the polarization can be neglected for engineering purposes.

F. Conclusions

Two methods have been used in this section to solve the problem of a finite dipole in an infinite dielectric rod. The first is an entirely numerical method. Excellent results have been obtained as compared with experimental data. Theoretically speaking, there is no limitation on the length of the antenna. However, for longer antennas, more points should be taken in order to have a reasonably accurate solution. A limitation exists in the number of storage locations available in a computer. For I. B. M. computer 7094, fifty mesh points taken on a dielectric-coated antenna is close to the upper limit. This method certainly is not confined only to this particular problem. Actually, it can be used to solve any kind of finite cylindrical antenna problem, once its Green's function is known. The second method, approximating the current by two terms, gives only a fairly good solution, and is applicable when the antenna is not too long, say $k_c z < \pi$. Its advantage is its analytic form, which is useful for practical purposes either in design or in the calculation of field patterns.

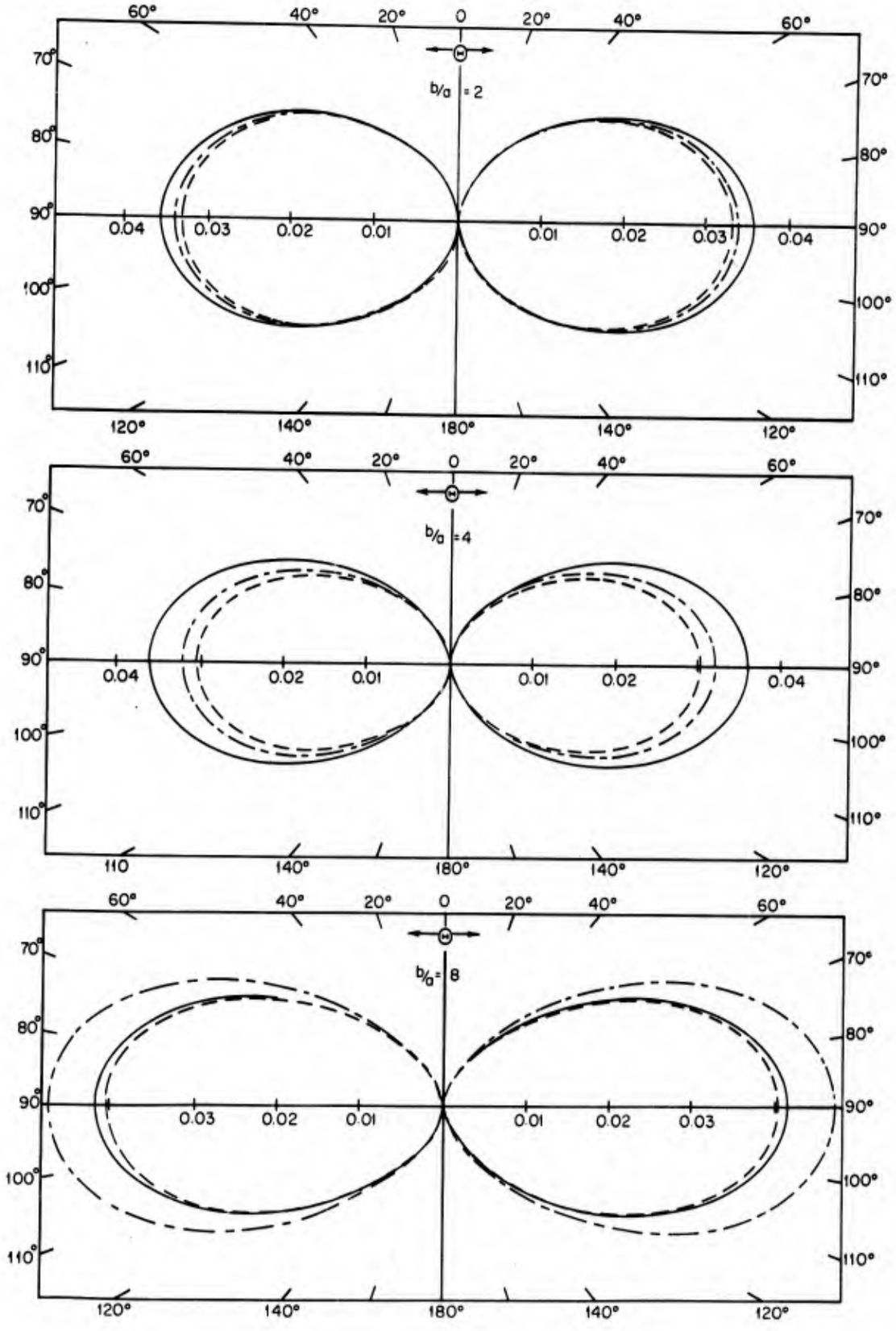

(a)——— BY NUMERICAL SOLUTION

(b)—·—·— BY TWO-TERM SOLUTION

(c)– – – – – BY TWO-TERM SOLUTION EXCLUDING POLARIZATION

FIG. 16 FIELD PATTERNS $\epsilon_r = 3.0$, $k_0 a = 0.04$, $k_0 h = \frac{3}{4}\pi$

Finally, no matter how complicated the mathematics may be, for engineering purposes, a dielectric-coated finite cylindrical antenna can be treated simply as a free-space dipole. The imaginary part of the current is well represented by a sine term, the real part by a shifted cosine term, both with Goubau surface-wave numbers rather than the free-space wave numbers. The field pattern can be calculated with the free-space Green's function as in the case of a conventional free-space dipole.

APPENDIX 1

The power associated with the surface wave transmission mode in a dielectric-coated infinite cylindrical antenna can also be calculated by integrating the appropriate part of the Poynting vector over two large surfaces perpendicular to the cylinder. That is

$$P_s = R_e \left\{ 2\pi \int_a^b r E^s_{1r} H^{s*}_{1\theta}\, dr + 2\pi \int_b^\infty r E^s_{2r} H^{s*}_{2\theta}\, dr \right\}$$

$$= P_{1s} + P_{2s} \qquad \text{(A-1)}$$

where a factor 2 is involved since power is transferred in both +z and -z directions. The first part of (A-1), P_{1s} is the power in the dielectric medium, and the second part of (A-1), P_{2s} is the power in free space. The field components E^s_{1r}, $H^s_{1\theta}$, E^s_{2r}, $H^s_{2\theta}$ are obtained from the residue term in the inverse Fourier transform. Following (20), (21), (22), and (23) in Section I, they are

$$E^s_{1r} = \frac{2Vk_s e^{ik_s z}}{\pi \xi F(k_s)} [A(k_s)J_1(\xi r) - B(k_s)Y_1(\xi r)] \qquad \text{(A-2)}$$

$$E^s_{2r} = \frac{4\epsilon_r k_s V e^{ik_s z}}{\pi^2 b \xi F(k_s)} K_1(\beta r) \qquad \text{(A-3)}$$

$$H^s_{1\theta} = -\frac{2V\omega\epsilon_1 e^{ik_s z}}{\pi \xi F(k_s)} [A(k_s)J_1(\xi r) - B(k_s)Y_1(\xi r)] \qquad \text{(A-4)}$$

$$H^s_{2\theta} = -\frac{4\omega\epsilon_1 V e^{ik_s z}}{\pi^2 b \xi F(k_s)} K_1(\beta r) \qquad \text{(A-5)}$$

where

$$A(k_s) = \xi K_1(\beta b)Y_o(\xi b) + \epsilon_r \beta K_o(\beta b)Y_1(\xi b) \tag{A-6}$$

$$B(k_s) = \xi K_1(\beta b)J_o(\xi b) + \epsilon_r \beta K_o(\beta b)J_1(\xi b) \tag{A-7}$$

$$\xi = \sqrt{k_1^2 - k_s^2} \qquad \beta = \sqrt{k_s^2 - k_o^2} \tag{A-8}$$

and $F(k_s)$, which is $\left[\frac{d}{dk} D(k)\right]_{k=-k_s}$, can be expressed as

$$F(k_s) = \frac{2k_s a}{\pi \xi} [A(k_s)J_1(\xi a) - B(k_s)Y_1(\xi a)]$$

$$+ \frac{2k_s b}{\pi K_1(\beta b)} [J_o(\xi a)Y_1(\xi b) - J_1(\xi b)Y_o(\xi a)]$$

$$\times \left\{ 2 \frac{\epsilon_r}{\beta b} K_o(\beta b)K_1(\beta b)\left(1 + \frac{\beta^2}{\xi^2}\right) + [K_1(\beta b)]^2(1 - \epsilon_r) + \epsilon_r [K_o(\beta b)]^2 \left(1 + \frac{\epsilon_r \beta^2}{\xi^2}\right) \right\} \tag{A-9}$$

Note that in deriving (A-9), some important equalities involving A(k) and B(k) are used. They are

$$A(k_s)J_1(\xi b) - B(k_s)Y_1(\xi b) = \frac{2}{\pi b} K_1(\beta b) \tag{A-10}$$

$$A(k_s)J_o(\xi b) - B(k_s)Y_o(\xi b) = -\frac{2\epsilon_r \beta}{\pi b \xi} K_o(\beta b) \tag{A-11}$$

$$A(k_s)J_o(\xi a) - B(k_s)Y_o(\xi a) = 0 \tag{A-12}$$

Following (A-12), it can also be proved that

$$A(k_s)J_1(\xi a) - B(k_s)Y_1(\xi a) = -\frac{4K_1(\beta b)}{\pi^2 \xi ab[J_o(\xi a)Y_1(\xi b) - J_1(\xi b)Y_o(\xi a)]} \tag{A-13}$$

If (A-13) is substituted in (A-9), $F(k_s)$ becomes

$$F(k_s) = -\frac{2k_s a}{\pi\xi}[A(k_s)J_1(\xi a) - B(k_s)Y_1(\xi a)]$$

$$+ \frac{8k_s}{\pi^3 \xi a} \frac{\left\{2\frac{\epsilon_r}{\beta b}K_o(\beta b)K_1(\beta b)(1+\frac{\beta^2}{\xi^2}) + [K_1(\beta b)]^2(1-\epsilon_r) + \epsilon_r[K_o(\beta b)]^2(1+\frac{\epsilon_r\beta^2}{\xi^2})\right\}}{[A(k_s)J_1(\xi a) - B(k_s)Y_1(\xi a)]} \tag{A-14}$$

If the field components E^s_{1r}, $H^s_{1\theta}$, E^s_{2r}, $H^s_{2\theta}$ are substituted in (A-1) and the integration is carried out with the help of the formulas in [10](p. 90), together with the relations (A-10), (A-11), and (A-12), the results are

$$P_{1s} = -\frac{8V^2\omega k_s \epsilon_1}{\pi\xi^2[F(k_s)]^2}\int_a^b \{A^2(k_s)r[J_1(\xi r)]^2 - 2A(k_s)B(k_s)rJ_1(\xi r)Y_1(\xi r) + B^2(k_s)r[Y_1(\xi r)]^2\}dr$$

$$= -\frac{16V^2\omega k_s \epsilon_1}{\pi^3\xi^2[F(k_s)]^2}\left\{[K_1(\beta b)]^2 + \frac{\epsilon_r^2\beta^2}{\xi^2}[K_o(\beta b)]^2 + \frac{2\epsilon_r\beta}{\xi^2 b}K_o(\beta b)K_1(\beta b) - \frac{\pi^2 a^2}{4}[A(k_s)J_1(\beta a) - B(k_s)Y_1(\beta a)]^2\right\} \tag{A-15}$$

$$P_{2s} = -\frac{32V^2\omega\epsilon_1 k_s}{\pi^3 b^2 \xi^2 [F(k_s)]^2} \int_b^\infty \epsilon_r r[K_1(\beta r)]^2 \, dr$$

$$= -\frac{16V^2\omega\epsilon_1 k_s}{\pi^3 \xi^2 [F(k_s)]^2} \left\{\epsilon_r[K_o(\beta b)]^2 + \frac{2\epsilon_r}{\beta b} K_o(\beta b)K_1(\beta b) - \epsilon_r[K_1(\beta b)]^2\right\} \tag{A-16}$$

When (A-15) and (A-16) are added, the total power associated with surface wave transmission is

$$P_s = -\frac{16V^2\omega\epsilon_1 k_s}{\pi^3 \xi^2 [F(k_s)]^2} \left\{\epsilon_r[K_o(\beta b)]^2\left(1 + \frac{\epsilon_r\beta^2}{\xi^2}\right) + [K_1(\beta b)]^2(1 - \epsilon_r)\right.$$

$$\left. + \frac{2\epsilon_r}{\beta b} K_o(\beta b)K_1(\beta b)\left(1 + \frac{\beta^2}{\xi^2}\right) - \frac{\pi^2 a^2}{4}[A(k_s)J_1(\xi a) - B(k_s)Y_1(\xi a)]^2\right\} \tag{A-17}$$

With the help of (A-14), (A-17) can be written alternatively as

$$P_s = -\frac{2\omega\epsilon_1 a V^2}{\xi F(k_s)} [A(k_s)J_1(\xi a) - B(k_s)Y_1(\xi a)] \tag{A-18}$$

Equation (A-18) is precisely the same as (23) in Section I.

APPENDIX 2

The power radiated from a dielectric-coated infinite cylindrical antenna can also be obtained from the integration of the normal component of the Poynting vector (50) in Section II over a great sphere. Owing to symmetry, it is possible to write the radiated power as follows:

$$P_r = 4\pi R^2 \int_0^{\frac{\pi}{2}} S \sin\theta \, d\theta \qquad \text{(A-19)}$$

where S is the Poynting vector. With (50) of Section II, (A-19) becomes

$$P_r = \frac{8k_1^2 \epsilon_r V^2}{\pi^3 b^2} \sqrt{\frac{\epsilon_o}{\mu_o}} \int_0^{\frac{\pi}{2}} \left| \frac{1}{\xi D(k)} \right|^2_{k=-k_o \cos\theta} \sin\theta \, d\theta \qquad \text{(A-20)}$$

After the transformation $x = k_o \cos\theta$, $dx = -k_o \sin\theta \, d\theta$ has been made, the following is obtained:

$$P_r = \frac{8\omega\epsilon_1 \epsilon_r V^2}{\pi^3 b^2} \int_0^{k_o} \frac{dx}{(k_1^2 - x^2) \, |D(-x)|^2} \qquad \text{(A-21)}$$

where $|D(-x)|^2 = [A(\sqrt{k_1^2 - x^2}, \sqrt{k_o^2 - x^2})]^2 + [B(\sqrt{k_1^2 - x^2}, \sqrt{k_o^2 - x^2})]^2$

A and B are defined by (42-a) and (42-b) in Section II. Equation (A-21) is indeed the same as (55) in Section II.

APPENDIX 3

The explicit formulas for calculating the constants, μ given by (28) in Section III, are listed below:

$$\mu_1(0) = -2R(1 - \cos k_1 t) - 2\int_o^{k_o t} M(\omega)\,\frac{1-\cos\omega}{\omega}\,d\omega + 2\int_o^{\infty} N(\omega)\,\frac{1-e^{-\omega}}{\omega}\,d\omega + i2R\sin k_1 t + i2\int_o^{k_o t} M(\omega)\,\frac{\sin\omega}{\omega}\,d\omega \qquad \text{(A-22)}$$

$$\mu_1(mt) = -2R\sin(k_1 t)\sin(mk_1 t) - 2\int_o^{k_o t} M(\omega)\,\frac{\sin\omega\sin(m\omega)}{\omega}\,d\omega + \int_o^{\infty} N(\omega)\,\frac{1-e^{-2\omega}}{\omega}\,e^{-(m-1)\omega}\,d\omega + i2R\sin(k_1 t)\cos(mk_1 t) + i2\int_o^{k_o t} M(\omega)\,\frac{\sin\omega\cos(m\omega)}{\omega}\,d\omega \qquad \text{(A-23)}$$

$$m = 1, 2, \ldots 4\ell-1$$

$$\mu_2(0) = 0 \tag{A-24}$$

$$\mu_2(mt) = 2R\frac{\sin(k_1t) - k_1t\cos(k_1t)}{k_1t}\cos(mk_1t)$$

$$+ 2\int_0^{k_ot} M(\omega)\frac{\sin\omega - \omega\cos\omega}{\omega^2}\cos(m\omega)\,d\omega$$

$$+\int_0^{\infty} N(\omega)\frac{(\omega-1) + (\omega+1)e^{-2\omega}}{\omega^2}e^{-(m-1)\omega}\,d\omega$$

$$+ i2R\frac{\sin(k_1t) - k_1t\cos(k_1t)}{k_1t}\sin(mk_1t)$$

$$+ i2\int_0^{k_ot} M(\omega)\frac{\sin\omega - \omega\cos\omega}{\omega^2}\sin(m\omega)\,d\omega \tag{A-25}$$

$$m = 1,\ 2,\ \ldots\ 4\ell\text{-}1$$

$$\mu_3(0) = 2R\frac{k_1^2t^2\cos(k_1t) - 2k_1t\sin(k_1t) - 2\cos(k_1t) + 2}{k_1^2t^2}$$

$$+ 2\int_0^{k_ot} M(\omega)\frac{\omega^2\cos\omega - 2\omega\sin\omega - 2\cos\omega + 2}{\omega^3}\,d\omega$$

$$+ 2\int_0^{\infty} N(\omega)\frac{2 - e^{-\omega}(\omega^2 + 2\omega + 2)}{\omega^3}\,d\omega$$

$$+ i2R\frac{k_1^2t^2\sin(k_1t) + 2k_1t\cos(k_1t) - 2\sin(k_1t)}{k_1^2t^2}$$

$$+ i2\int_0^{k_ot} M(\omega)\frac{\omega^2\sin\omega + 2\omega\cos\omega - 2\sin\omega}{\omega^3}\,d\omega \tag{A-26}$$

$$\mu_3(mt) = -2R\,\frac{k_1^2t^2\sin(k_1t) + 2k_1t\cos(k_1t) - 2\sin(k_1t)}{k_1^2t^2}\,\sin(mk_1t)$$

$$- 2\int_o^{k_ot} M(\omega)\,\frac{\omega^2\sin\omega + 2\omega\cos\omega - 2\sin\omega}{\omega^3}\,\sin(m\omega)\,d\omega$$

$$+\int_o^{\infty} N(\omega)\,\frac{(\omega^2 - 2\omega + 2) - (\omega^2 + 2\omega + 2)\,e^{-2\omega}}{\omega^3}\,e^{-(m-1)\omega}\,d\omega$$

$$+ i2R\,\frac{k_1^2t^2\sin(k_1t) + 2k_1t\cos(k_1t) - 2\sin(k_1t)}{k_1^2t^2}\,\cos(mk_1t)$$

$$+ i2\int_o^{k_ot} M(\omega)\,\frac{\omega^2\sin\omega + 2\omega\cos\omega - 2\sin\omega}{\omega^3}\,\cos(m\omega)\,d\omega \qquad (A\text{-}27)$$

$$m = 1,\ 2,\ \ldots\ 4\ell - 1$$

where $$R = \frac{2\epsilon_r\sqrt{k_1^2 - k_o^2}\,b\,K_o(\sqrt{k_1^2 - k_o^2}\,b)}{(k_1b)^2\,[2K_1(\sqrt{k_1^2 - k_o^2}\,b) + \epsilon_r\sqrt{k_1^2 - k_o^2}\,b\,K_o(\sqrt{k_1^2 - k_o^2}\,b)]} \qquad (A\text{-}28)$$

$M(\omega)$ and $N(\omega)$ are defined by

$$M(\omega) = \frac{4\epsilon_r J_o^2(Qa)}{\pi^2\{Qb J_o(Qb)J_1(Pb) - \epsilon_r Pb J_1(Qb)J_o(Pb)]^2 + [Qb J_o(Qb)Y_1(Pb) - \epsilon_r Pb J_1(Qb)Y_o(Pb)]^2\}} \qquad (A\text{-}29)$$

$$N(\omega) = \frac{4\epsilon_r J_o^2(Va)}{\pi^2\{[Vb J_o(Vb)J_1(Ub) - \epsilon_r Ub J_1(Vb)J_o(Ub)]^2 + [Vb J_o(Vb)Y_1(Ub) - \epsilon_r Ub J_1(Vb)Y_o(Ub)]^2\}} \qquad (A\text{-}30)$$

and $$P = \sqrt{k_o^2 - \frac{\omega^2}{t^2}}$$

$$Q = \sqrt{k_1^2 - \frac{\omega^2}{t^2}}$$

$$U = \sqrt{k_o^2 + \frac{\omega^2}{t^2}}$$

$$V = \sqrt{k_1^2 + \frac{\omega^2}{t^2}} \qquad \text{(A-31)}$$

APPENDIX 4

Explicit formulas for the Ψ's defined by (32), (33), (34), and (35) in Section III are listed as follows:

$$\Psi_v = -2\int_0^{k_o h} M'(\omega)\,\frac{k_s h \sin\omega(\cos\omega - \cos k_s h)}{k_s^2 h^2 - \omega^2}\,d\omega + \int_0^{\infty} N'(\omega)\,\frac{k_s h(1+e^{-2\omega} - 2e^{-\omega}\cos k_s h)}{k_s^2 h^2 + \omega^2}\,d\omega + i2\int_0^{k_o h} M'(\omega)\,\frac{k_s h\cos\omega(\cos\omega - \cos k_s h)}{k_s^2 h^2 - \omega^2}\,d\omega \qquad (A-32)$$

$$\Psi_u = -2\int_0^{k_o h} M'(\omega)\,\frac{k_s h \sin\omega(\omega\cos\omega\sin k_s h - k_s h\sin\omega\cos k_s h)}{\omega(k_s^2 h^2 - \omega^2)}\,d\omega + \int_0^{\infty} N'(\omega)\,\frac{k_s h[\omega\sin k_s h(1+e^{-2\omega}) - k_s h\cos k_s h(1-e^{-2\omega})]}{\omega(k_s^2 h^2 + \omega^2)}\,d\omega + i2\int_0^{k_o h} M'(\omega)\,\frac{k_s h\cos\omega(\omega\cos\omega\sin k_s h - k_s h\sin\omega\cos k_s h)}{\omega(k_s^2 h^2 - \omega^2)}\,d\omega \qquad (A-33)$$

Let the four new quantities A, B, C, and D be defined as follows:

$$A = \int_{-h}^{h} M_{oz'} \mathcal{K}_d(o, z')\, dz' = \int_{o}^{k_o h} M'(\omega) \frac{2k_s h(\omega \sin k_s h - k_s h \sin \omega)}{k_s^2 h^2 - \omega^2} d\omega$$

$$+ \int_{o}^{\infty} N'(\omega) \frac{2(k_s h e^{-\omega} - k_s h \cos k_s h + \omega \sin k_s h)}{k_s^2 h^2 + \omega^2} d\omega$$

$$+ i \int_{o}^{k_o h} M'(\omega) \frac{2k_s h (\cos \omega - \cos k_s h)}{k_s^2 h^2 - \omega^2} d\omega - \Psi_v \qquad \text{(A-34)}$$

$$B = \int_{-h}^{h} M_{oz'} \mathcal{K}_d(\omega\omega, z')\, dz' = \int_{o}^{k_o h} M'(\omega) \frac{2[\omega + k_s h \cos k_s h \sin(\omega\omega) - k_s h \sin \omega \cos(\omega\omega)]}{k_s^2 h^2 - \omega^2} d\omega$$

$$+ \int_{o}^{\infty} N'(\omega) \frac{2[\omega + k_s h e^{-\omega} \cosh(\omega\omega) - k_s h \cos k_s h e^{-\omega\omega}]}{k_s^2 h^2 + \omega^2} d\omega$$

$$+ i \int_{o}^{k_o h} M'(\omega) \frac{2k_s h \cos(\omega\omega)(\cos \omega - \cos k_s h)}{k_s^2 h^2 - \omega^2} d\omega - \Psi_v$$

(A-35)

$$C = \int_{-h}^{h} F_{oz'} \mathcal{K}_d(0, z')\, dz'$$

$$= \int_{o}^{k_o h} M'(\omega) \frac{2[\omega^2(1 - \cos k_s h) - k_s h \omega \sin \omega \sin k_s h - k_s^2 h^2 \cos k_s h(\cos \omega - 1)]}{\omega(k_s^2 h^2 - \omega^2)} d\omega$$

$$+ \int_{o}^{\infty} N'(\omega) \frac{2[\omega^2(1 - \cos k_s h) - k_s^2 h^2 \cos k_s h + k_s h e^{-\omega}(\omega \sin k_s h + k_s h \cos k_s h)]}{\omega(k_s^2 h^2 + \omega^2)} d\omega$$

$$+ i \int_{o}^{k_o h} M'(\omega) \frac{2k_s h(\omega \cos \omega \sin k_s h - k_s h \sin \omega \cos k_s h)}{\omega(k_s^2 h^2 - \omega^2)} d\omega - \Psi_u$$

(A-36)

$$D = \int_{-h}^{h} F_{oz'} \kappa_d (\omega\omega, z')\, dz'$$

$$= \int_{o}^{k_o h} M'(\omega) \frac{2[\omega^2(\sin k_s h - \cos k_s h) + k_s^2 h^2 \cos k_s h - k_s h \cos(\omega\omega)(\omega \sin\omega \sin k_s h + k_s h \cos\omega \cos k_s h)]}{\omega(k_s^2 h^2 - \omega^2)} d\omega$$

$$+ \int_{o}^{\infty} N'(\omega) \frac{2[\omega^2(\sin k_s h - \cos k_s h) - k_s^2 h^2 \cos k_s h + k_s h e^{-\omega} \cosh(\omega\omega)(\omega \sin k_s h + k_s h \cos k_s h)]}{\omega(k_s^2 h^2 + \omega^2)} d\omega$$

$$+ i \int_{o}^{k_o h} M'(\omega) \frac{2k_s h \cos(\omega\omega)(\omega \cos\omega \sin k_s h - k_s h \sin\omega \cos k_s h)}{\omega(k_s^2 h^2 - \omega^2)} d\omega - \Psi_u \qquad \text{(A-37)}$$

Then,

$$\Psi_{dvv} = \frac{(1 - \cos k_s h)B - (\sin k_s h - \cos k_s h)A}{1 - \cos k_s h - \sin k_s h (\sin k_s h - \cos k_s h)} \qquad \text{(A-38)}$$

$$\Psi_{dvu} = \frac{A - \sin k_s h\, B}{1 - \cos k_s h - \sin k_s h (\sin k_s h - \cos k_s h)} \qquad \text{(A-39)}$$

$$\Psi_{duv} = \frac{(1 - \cos k_s h)D - (\sin k_s h - \cos k_s h)C}{1 - \cos k_s h - \sin k_s h (\sin k_s h - \cos k_s h)} \qquad \text{(A-40)}$$

$$\Psi_{duu} = \frac{C - \sin k_s h\, D}{1 - \cos k_s h - \sin k_s h (\sin k_s h - \cos k_s h)} \qquad \text{(A-41)}$$

where $$\omega\omega = \omega\left(1 - \frac{\pi}{2k_s h}\right) \qquad \text{(A-42)}$$

$$M'(\omega) = \frac{4\varepsilon_r (k_s/k_o)^2 (k_1^2 h^2 - \omega^2) J_o^2(Qa)}{\pi^2 (k_s^2 h^2 - \omega^2)\{[QbJ_o(Qb)J_1(Pb) - \varepsilon_r PbJ_1(Qb)J_o(Pb)]^2 + [QbJ_o(Qb)Y_1(Pb) - \varepsilon_r PbJ_1(Qb)Y_o(Pb)]^2\}} \quad \text{(A-43)}$$

$$N'(\omega) = \frac{4\varepsilon_r (k_s/k_o)^2 (k_1^2 h^2 + \omega^2) J_o^2(Va)}{\pi^2 (k_s^2 h^2 + \omega^2)\{[VbJ_o(Vb)J_1(Ub) - \varepsilon_r UbJ_1(Vb)J_o(Ub)]^2 + [VbJ_o(Vb)Y_1(Ub) - \varepsilon_r UbJ_1(Vb)Y_o(Ub)]^2\}} \quad \text{(A-44)}$$

and

$$P = \sqrt{k_o^2 - \frac{\omega^2}{h^2}}$$

$$Q = \sqrt{k_1^2 - \frac{\omega^2}{h^2}}$$

$$U = \sqrt{k_o^2 + \frac{\omega^2}{h^2}}$$

$$V = \sqrt{k_1^2 + \frac{\omega^2}{h^2}} \quad \text{(A-45)}$$

ACKNOWLEDGEMENT

The author wishes to thank Professor R. W. P. King for his suggestion of this problem, helpful discussion, reading and correcting the manuscript, and above all his encouragement throughout the course of this research.

The author also thanks Professor T. T. Wu, Dr. Chin-Lin Chen, and Mr. David Chang for their stimulating discussion and comments, and Mr. David Lamensdorf for his valuable experimental data.

REFERENCES

[1] Wu, T. T. "Theory of Dipole Antenna and the Two Wire Transmission Line," J. of Math. Phys., Vol. 2, No. 4 (July-August, 1961), pp. 550-574.

[2] Peterson, Gunnar. "The Current Distribution on Infinite Antennas with and without a Dielectric Coating," Transactions of Royal Institute of Technology, Stockholm, Sweden, (1965), Nr 241.

[3] Goubau, Georg. "Surface Waves and Their Application to Transmission Line" J. Appl. Phys., Vol. 21 (1950), pp. 1119-1128.

[4] Goubau, Georg. "Single Conductor Surface Wave Transmission Lines," Proc. IRE, Vol. 39 (June 1951), pp. 619-624.

[5] Duncan, R. H. "Theory of the Infinite Cylindrical Antenna Including the Feedpoint Singularity in Antenna Current," J. of Research, NBS, Vol. 66D, No. 2 (March-April, 1962), pp. 181-188.

[6] Wu, T. T. and R. W. P. King. "Driving Point and Input Admittance of Linear Antenna," J. Appl. Phys., Vol. 30, No. 1 (1959), p. 74.

[7] Kuehl, Hans H. "Current on an Infinitely Long Cylindrical Antenna," J. of Math. and Phys., Vol. 39 (July, 1960), p. 121.

[8] Kunz, K. S. "Asymptotic Behavior of the Current on an Infinite Cylindrical Antenna," J. of Research, NBS, Vol. 67D (July-August 1963), p. 417.

[9] Papas, Charles H. "On the Infinitely Long Cylindrical Antenna," J. Appl. Phys., Vol. 20 (May, 1949), pp. 437-440.

[10] Bateman, Harry. Higher Transcendental Functions. (Vol. 2) New York, Toronto and London: McGraw-Hill, 1953.

[11] Jackson, John D. Classical Electrodynamics. New York: Wiley, 1962.

[12] Young, Andrew. "Approximate Product Integration," Proc. Royal Soc., Vol. A224 (1954), pp. 552-561.

[13] Young, Andrew. "The Application of Approximate Product-Integration to the Numerical Solution of Integral Equations," Proc. Royal Soc., Vol. A224 (1954), pp. 561-573.

[14] King, R. W. P. The Theory of Linear Antennas. Cambridge, Massachusetts: Harvard University Press, 1956.

[15] King, R. W. P. "Linear Arrays: Currents, Impedances, and Fields, I," IRE Transactions on Antennas and Propagation, Vol. AP-7 Special Supplement (December, 1959), pp. s-440--s-457.

[16] Lamensdorf, David. "An Experimental Investigation of Dielectric Coated Antennas," Cruft SR 13.

Unclassified

Security Classification

DOCUMENT CONTROL DATA - R&D

(Security classification of title, body of abstract and indexing annotation must be entered when the overall report is classified)

1. ORIGINATING ACTIVITY *(Corporate author)*
Cruft Laboratory
Division of Engineering and Applied Physics
Harvard University, Cambridge, Massachusetts

2a. REPORT SECURITY CLASSIFICATION
Unclassified

2b. GROUP

3. REPORT TITLE

A THEORETICAL STUDY OF DIELECTRIC-COATED CYLINDRICAL ANTENNAS

4. DESCRIPTIVE NOTES *(Type of report and inclusive dates)*
Interim technical report

5. AUTHOR(S) *(Last name, first name, initial)*
Chung-Yu Ting

6. REPORT DATE	7a. TOTAL NO. OF PAGES	7b. NO. OF REFS
July, 1966	88	16

8a. CONTRACT OR GRANT NO.	9a. ORIGINATOR'S REPORT NUMBER(S)
Nonr-1866(32)	Cruft Laboratory Technical Report No. 506
b. PROJECT NO. NR-371-016	
c.	9b. OTHER REPORT NO(S) *(Any other numbers that may be assigned this report)*
d.	

10. AVAILABILITY/LIMITATION NOTICES

Reproduction in whole or in part is permitted by the U. S. Government. Distribution of this document is unlimited.

11. SUPPLEMENTARY NOTES	12. SPONSORING MILITARY ACTIVITY
Research supported in part by Div. of Engineering and Appl. Phys., Harvard University, Cambridge, Massachusetts	Joint Services Electronics Program

13. ABSTRACT

A cylindrical antenna, either infinite or finite, which is imbedded in a concentric dielectric rod has been investigated by employing a rigorous formulation. The infinite case is solved easily by a Fourier transform method; the finite case is solved first by a numerical method, then by a two-term approximation. The mathematical analysis is intricate, nevertheless, the results obtained for the finite antenna are as simple as for the free-space dipole. It is shown in both cases that the input conductances are larger than for the corresponding free-space antennas, and the field patterns tend to be more broadside. The method is applicable regardless of the thicknesses of the antennas and the dielectric rod. This study is limited to thin antennas in rather thick dielectric cylinders. However, the dielectric rod is still not thick enough to support a T. M. mode.

DD FORM 1 JAN 64 1473

Unclassified

Security Classification

14. KEY WORDS	LINK A		LINK B		LINK C	
	ROLE	WT	ROLE	WT	ROLE	WT
Infinite dielectric-coated cylindrical antenna Transmission current Radiation current Transmission efficiency Radiation efficiency Finite dielectric-coated cylindrical antenna Current distribution Two-term approximation Field pattern						

INSTRUCTIONS

1. **ORIGINATING ACTIVITY:** Enter the name and address of the contractor, subcontractor, grantee, Department of Defense activity or other organization *(corporate author)* issuing the report.

2*a*. **REPORT SECURITY CLASSIFICATION:** Enter the overall security classification of the report. Indicate whether "Restricted Data" is included. Marking is to be in accordance with appropriate security regulations.

2*b*. **GROUP:** Automatic downgrading is specified in DoD Directive 5200.10 and Armed Forces Industrial Manual. Enter the group number. Also, when applicable, show that optional markings have been used for Group 3 and Group 4 as authorized.

3. **REPORT TITLE:** Enter the complete report title in all capital letters. Titles in all cases should be unclassified. If a meaningful title cannot be selected without classification, show title classification in all capitals in parenthesis immediately following the title.

4. **DESCRIPTIVE NOTES:** If appropriate, enter the type of report, e.g., interim, progress, summary, annual, or final. Give the inclusive dates when a specific reporting period is covered.

5. **AUTHOR(S):** Enter the name(s) of author(s) as shown on or in the report. Enter last name, first name, middle initial. If military, show rank and branch of service. The name of the principal author is an absolute minimum requirement.

6. **REPORT DATE:** Enter the date of the report as day, month, year; or month, year. If more than one date appears on the report, use date of publication.

7*a*. **TOTAL NUMBER OF PAGES:** The total page count should follow normal pagination procedures, i.e., enter the number of pages containing information.

7*b*. **NUMBER OF REFERENCES:** Enter the total number of references cited in the report.

8*a*. **CONTRACT OR GRANT NUMBER:** If appropriate, enter the applicable number of the contract or grant under which the report was written.

8*b*, 8*c*, & 8*d*. **PROJECT NUMBER:** Enter the appropriate military department identification, such as project number, subproject number, system numbers, task number, etc.

9*a*. **ORIGINATOR'S REPORT NUMBER(S):** Enter the official report number by which the document will be identified and controlled by the originating activity. This number must be unique to this report.

9*b*. **OTHER REPORT NUMBER(S):** If the report has been assigned any other report numbers *(either by the originator or by the sponsor)*, also enter this number(s).

10. **AVAILABILITY/LIMITATION NOTICES:** Enter any limitations on further dissemination of the report, other than those imposed by security classification, using standard statements such as:

(1) "Qualified requesters may obtain copies of this report from DDC."

(2) "Foreign announcement and dissemination of this report by DDC is not authorized."

(3) "U. S. Government agencies may obtain copies of this report directly from DDC. Other qualified DDC users shall request through

_____."

(4) "U. S. military agencies may obtain copies of this report directly from DDC. Other qualified users shall request through

_____."

(5) "All distribution of this report is controlled. Qualified DDC users shall request through

_____."

If the report has been furnished to the Office of Technical Services, Department of Commerce, for sale to the public, indicate this fact and enter the price, if known.

11. **SUPPLEMENTARY NOTES:** Use for additional explanatory notes.

12. **SPONSORING MILITARY ACTIVITY:** Enter the name of the departmental project office or laboratory sponsoring *(paying for)* the research and development. Include address.

13. **ABSTRACT:** Enter an abstract giving a brief and factual summary of the document indicative of the report, even though it may also appear elsewhere in the body of the technical report. If additional space is required, a continuation sheet shall be attached.

It is highly desirable that the abstract of classified reports be unclassified. Each paragraph of the abstract shall end with an indication of the military security classification of the information in the paragraph, represented as *(TS)*, *(S)*, *(C)*, or *(U)*.

There is no limitation on the length of the abstract. However, the suggested length is from 150 to 225 words.

14. **KEY WORDS:** Key words are technically meaningful terms or short phrases that characterize a report and may be used as index entries for cataloging the report. Key words must be selected so that no security classification is required. Identifiers, such as equipment model designation, trade name, military project code name, geographic location, may be used as key words but will be followed by an indication of technical context. The assignment of links, roles, and weights is optional.